2016

Provenance Analysis of Granite Cobbles in the Tiskilwa till Using U -pb Geochronology

Paul Antone Meister
Illinois State University, pameist@ilstu.edu

PROVENANCE ANALYSIS OF GRANITE COBBLES IN THE TISKILWA TILL USING U-PB GEOCHRONOLOGY

Paul A Meister

51 Pages

U-Pb isotopic ages were determined for zircons extracted from granitic and related rocks in the Tiskilwa till to determine their origin. Crystalline cobbles (n = 750) were collected at localities from each of the four of the sub-lobes of the terminal Wisconsin moraines. Two sites were chosen from the Decatur, Peoria, and Princeton sub-lobes with one sample taken from the Harvard sub-lobe. Each sample was then individually processed, the zircons handpicked (n = 301), and geochronology conducted using LA-MC-ICPMS at the University of Arizona Laserchron Center. A Kolmogorov-Smirnov (K-S) statistical analysis show that all samples have identical zircon age spectra with the populations being dominated by Archean age (>2.5 Ga) grains and peak age being 2.7 Ga. The dominance of Archean grains indicate a source located in the Superior Province, with the Hudson Bay Terrane (3.36 – 2.69 Ga) being the most likely source area for the granite clasts. In successfully utilizing granite clasts to determine provenance, this study could provide further insight into glacial transport systems.

KEYWORDS: Geochronology, Glacial Till, U-Pb, Zircon

PROVENANCE ANALYSIS OF GRANITE COBBLES IN THE TISKILWA TILL USING U-PB GEOCHRONOLOGY

PAUL A. MEISTER

A Thesis Submitted in Partial
Fulfillment of the Requirements
for the Degree of

MASTER OF SCIENCE

Department of Geography-Geology

ILLINOIS STATE UNIVERSITY

2016

PROVENANCE ANALYSIS OF GRANITE COBBLES IN THE TISKILWA TILL USING U-PB GEOCHRONOLOGY

PAUL A. MEISTER

COMMITTEE MEMBERS:

David H. Malone, Chair

Eric W. Peterson

Lisa Tranel

ACKNOWLEDGMENTS

The writer wishes to thank Dr. David Malone for his endless support during the research process as well as the assistance collecting samples and processing them. Dr. Eric Peterson, Dr. Lisa Tranel, and Dr. Tenley Banik for their invaluable input and support. Jason Thomason and Andy Stumpf for their input during the proposal process. Ellyn Rickels for the ideas and support during the research phase. Kasey Garber and Gwen Gates for their assistance processing the zircons. University of Arizona Laserchron center for being such gracious hosts during the data collecting process. Dr. John Craddock for his impromptu assistance in thesis defense and the field camp crew of 2016 for being such a willing and gracious audience. Lastly, his wife Heather for the tireless support and motivation to complete such an endeavor. I could not have done this without the support of each of you and for that I thank you!

P. A. M.

CONTENTS

TABLES

FIGURES

CHAPTER I

THE PROBLEM AND ITS BACKGROUND

INTRODUCTION

Glacial deposits in Illinois have been recognized since the late 1800's as forming landforms that are important for agriculture and natural resources such as sand and gravel deposits. The multiple glaciation events forming these landforms have been noted as far back as 1878 when T.C. Chamberlin mapped them, and described deposits of different ages (Chamberlin, 1878). With the recognition of multiple glacial events, it was determined that during the Wisconsin Episode a till, classified as the Tiskilwa Formation (Hansel and Johnson, 1996) (Figure 1.1), is one of the thickest tills in Illinois (Wickham *et. al.*, 1988). Of the four Wedron Formations, the Tiskilwa is the thickest and most areal extensive (Hansel and Johnson, 1996). The Tiskilwa Formation deposition began as the Laurentide ice sheet entered Illinois 29,000 YB (Curry *et al.*, 2011). During the subsequent advancement and retreat of the ice sheet, the Tiskilwa Formation was deposited in outcrops located in the outermost moraines of the Harvard, Princeton, Peoria, and Decatur sublobes (Figure 1.2). In these areas, the till can reach thicknesses of more than 60 m (200 ft) (Wickham *et al.*, 1988).

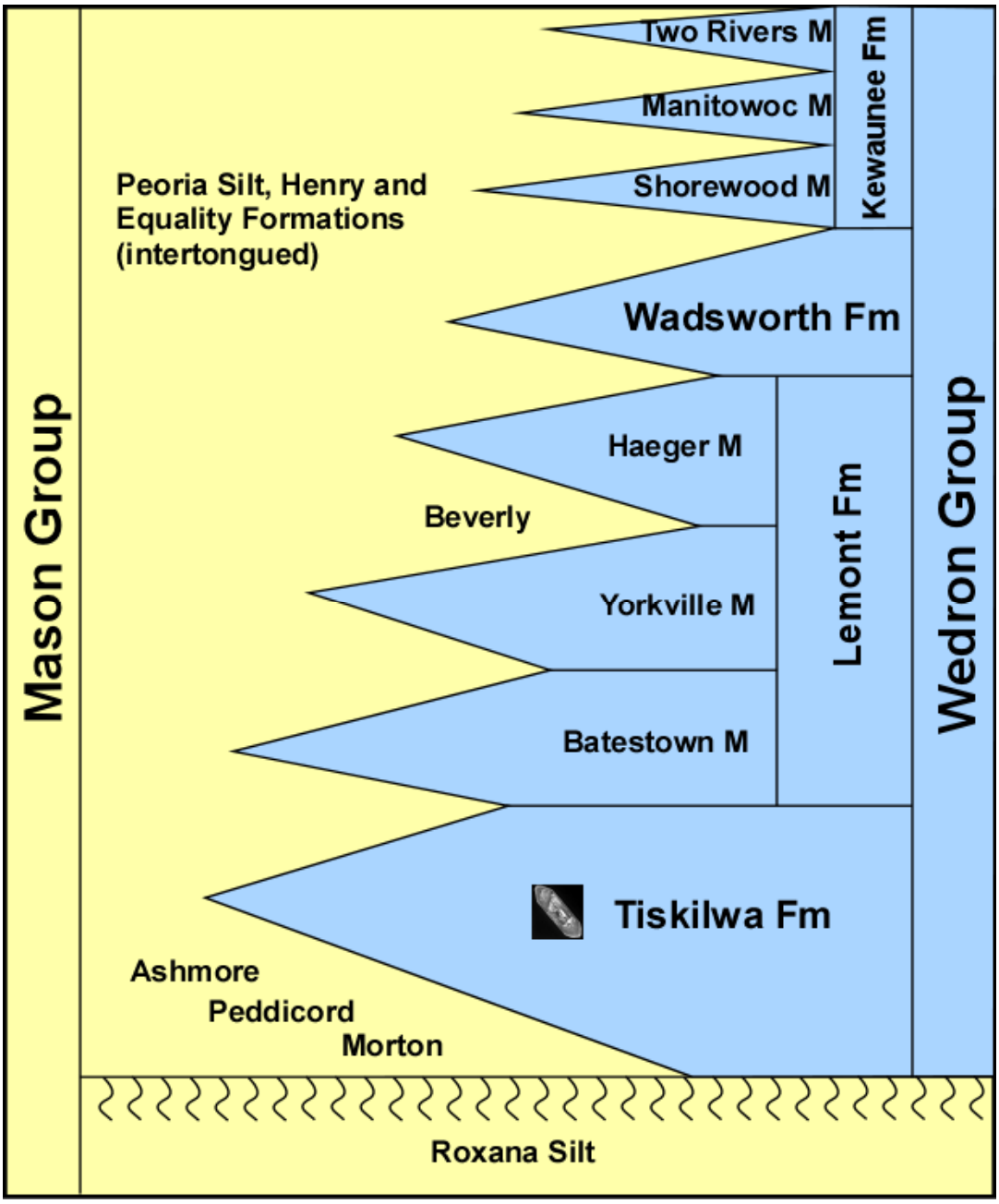

Figure 1.1: Lithostratigraphy of Wisconsin and Hudson Episodes in Illinois (modified from Hansel and Johnson, 1996)

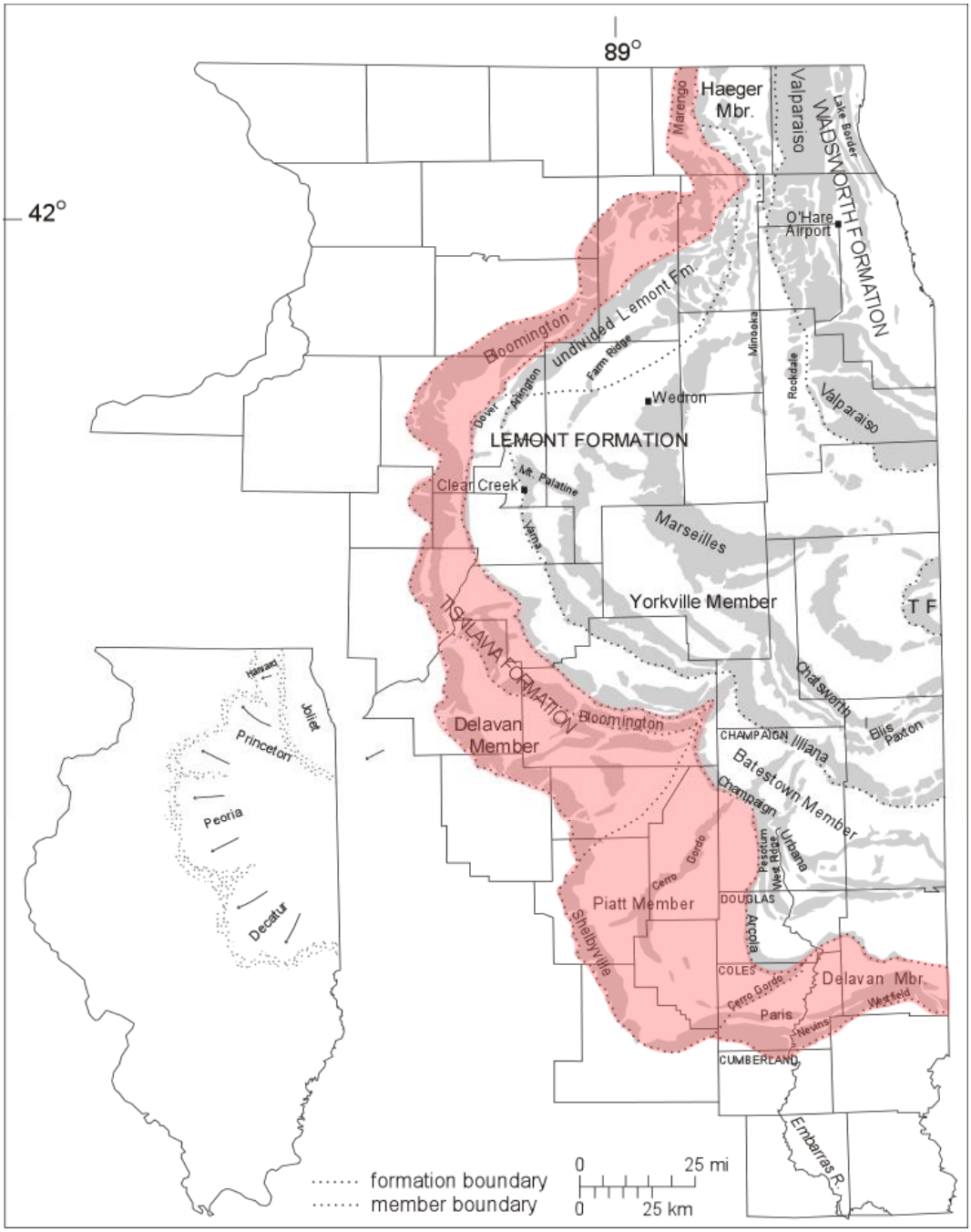

Figure 1.2: Map of Wisconsinan age moraines in Illinois with shading indicating Tiskilwa formation exposed at the surface (from Hansel and Johnson, 1996).

Leverett and Tayor (1915) were the first to recognize that the Tiskilwa and other Tills deposited during the Wisconsin Episode by an ice lobe that flowed through Lake Michigan. Their interpretation was based on the lobate shape of glacial moraines that parallel the current lake shore to the south and west. Hansel and Johnson (1992) determined that the Tiskilwa was deposited between 29,000-23,000 YBP during the Michigan Subepisode.

Later work by Willman and Frye (1970) divided the Lake Michigan into the Peoria and Decatur sublobes as "interlobate" in nature with the ice sheet that deposited the Peoria sub-lobe having a northerly source and the ice sheet that deposited the Decatur sub-lobe as having a more easterly source. Bleuer and McKay (1975) and Moore (1981) support the hypothesis of Leverett and Taylor of a more northerly source (Johnson *et. al.*, 1996). Johnson *et al.* (1986) used garnet-epidote ratios to determine that the Decatur and Peoria sub-lobes contained ratios that corresponded to the Southern and Superior Provinces (Figure 1.4).

Figure 1.3: Diagram of the Laurentide ice sheet with line work showing positions of the ice sheet and arrow indicating ide flow direction (from Leverett and Taylor, 1915).

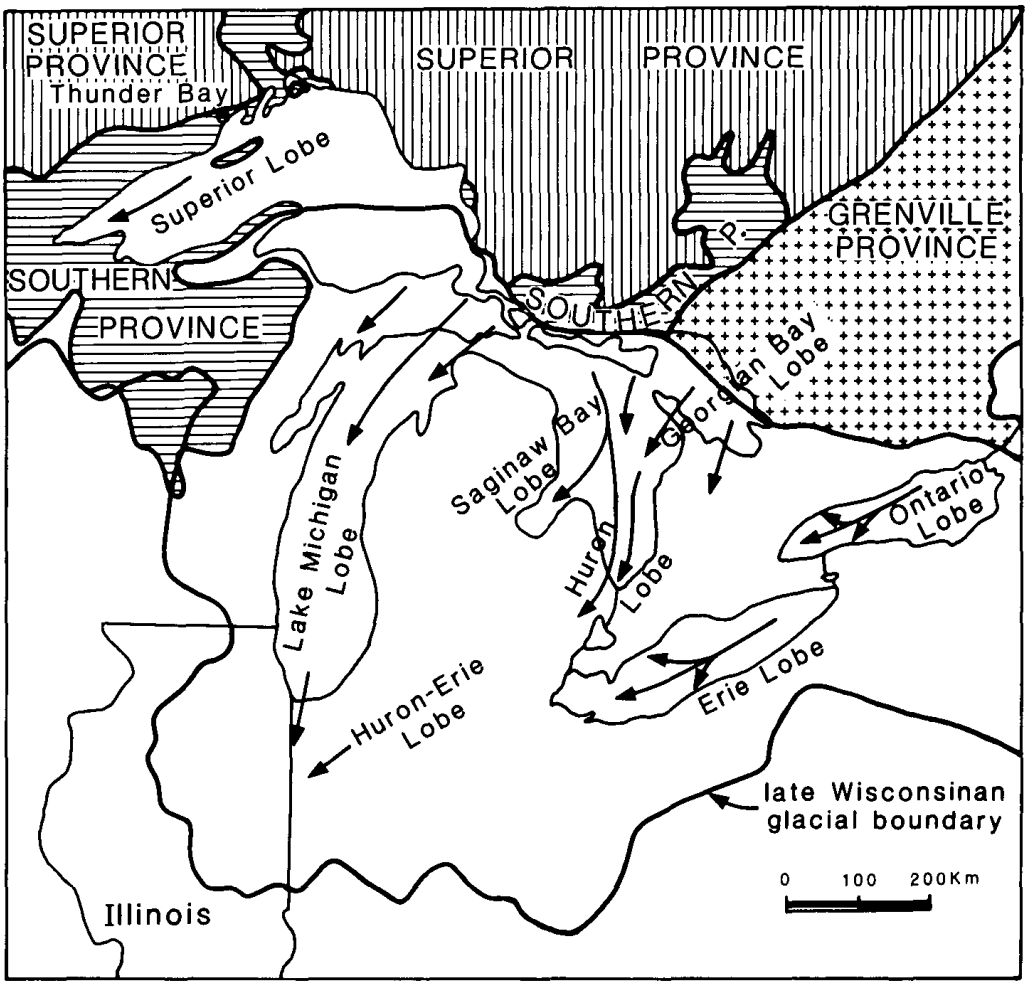

Figure 1.4: Diagram showing ice flow directions during Wisconsin Episode (Johnson *et. al.*, 1986).

LOCATION AND GEOLOGIC SETTING

This study was conducted over a large area of Illinois, at sites located on terminal moraines of four of the five major Wisconsin Episode sublobes of the Laurentide Ice Sheet (Figure 1.2). The sites are located in the Decatur sublobe to the south, the Peoria sublobe to the west, the Princeton sub-lobe to the northwest, and the Harvard sublobe to the north. To the east, the Huron-Erie sublobe was not sampled because glaciers flowing through the Huron and Erie lakes basins had a different source area and did not deposit

the Tiskilwa Formation till. The Joliet subloabe was not sampled due to the lack of till outcrop at the surface. The Laurentide ice sheet transported eroded bedrock that could originate from sources in the Superior, Southern, or Grenville structural provinces. At all the sites, the Tiskilwa Formation till was exposed at the land surface.

RESEARCH OBJECTIVES

The objective of this project is to determine if geochronology of glacial erratics from an end moraine on a regional scale can be successful in determining provenance. A second objective of the project is to compare ages obtained regionally with ages obtained from granite cobbles in a recessional moraine of the Peoria sublobe (Rickels, 2016).

SIGNIFICANCE

The significance of this study is two-fold. First and foremost, a regional isotopic provenance study on glacial till using granite cobbles has not been performed in Illinois. In fact, a regional study on granite clasts in glacial till at this scope has never been performed in the world. In many studies on glaciated terrain, only zircons from a few clasts have been dated to determine till provenance (e.g., Plouffe et al., 2011; Doornbos et al., 2009). By analyzing the age of several hundred clasts, the reliability of the dating will be drastically improved by reducing sampling bias. The increased sample size will reduce potential sampling error as well as increasing the data set acquired. Secondly, obtaining precise ages on zircons will lead to a refinement of sedimentary provenance for the Tiskilwa till.

HYPOTHESES

This project is designed to test the application of U/Pb geochronology on granite clasts for determining the provenance of a glacial till. The following hypotheses will be examined through the research.

1. U/Pb isotopes dating can provide ages of granite clasts in the Tiskilwa Formation till and thus lead to a refinement in source area determination.
2. U/Pb isotope dates may be used to distinguish between specific glacial lobes of the Wisconsin Episode and therefore could lead to revision of ice flow pathways.

CHAPTER II

REVIEW OF RELATED LITERATURE

GLACIAL TILL

Glacial till provenance has long been studied to further refine and constrain the geologic history and to determine the source areas for "exotic" or mineralized material. Various techniques have been used to determine the abundance of indicator minerals (McClenaghan *et al.* 2000; Averill 2001) and garnet and epidote grains (Gwyn and Dreimanis, 1979) in till for provenance studies. Others have used pebble lithologies to identify the source area of the till (e.g., Prest *et al*., 2000). Still others have used variance in matrix textures and composition (e.g., Lusardi *et al.,* 2011) and shape of mineral grains (Dreimanis and Vagners, 1971). These techniques can be used to identify a provenance region, however, they do not provide an emplacement or crystallization age of the source rock. More recently, U/Pb isotopes from zircons and $^{40}Ar/^{39}Ar$ isotopes from feldspars have been used to determine ages of crystalline glacial erratics (e.g., Doornbos *et al*. 2009; Roy *et al*. 2007). Using detrital zircons to determine provenance builds on the extensive use of the isotopes to date bedrock from both detrital sources (Malone *et al*., 2014a) and in-situ sources (Malone *et al*., 2014b) to successfully determine provenance. Doornbos *et al.* (2009) were successful in determining precise ages of glacial erratics transported across the western Arctic Archipelago of Canada using only eight erratics with an *in situ* method.

A combination of methodologies, including U/Pb isotopes with geophysical studies have also been used to trace mineralized erratics to the source bedrock (Plouffe *et.al.*, 2011).

Till Geochronology

Methods for till geochronology have included sampling sand size particles with mixed results. One such study performed recently by Licht *et al.* (2013) was successful in gathering U/Pb ages on till in Antarctica; however, they acknowledge that by collecting sand size particles there may have been recycling from previously exposed unsuccessful in using sand size particles to distinguish provenance.

Utilizing granite cobbles will lead to a more precise provenance on till. Sand sized particles likely contain detrital zircons from many sources while crystalline rocks would contain zircons that would have formed at the time of the rock formation. In fact, Zimmerman et al. (2015) show that sedimentary processes coupled with different transport mechanisms can produce large differences in provenance signals within a single sedimentary succession. Using only granite clasts will eliminate the difference in provenance signals.

SUPERIOR PROVINCE

Within the heart of the North American continent lies the Superior Province. Comprising a total area of 1.4 x 10^6 km^2, the Superior Province is the largest craton on Earth (Percival *et al.,* 2012). The Superior Province consists largely of Archean rocks >2500 Ma (Card and Ciesielski, 1986) which can be subdivided into four regions (Figure 2.1). The four regions are the western, central, moyen-nord. and northeastern Superior regions (Percival *et al.,* 2012). Located within the western region, the Hudson Bay Terrane is comprised of plutonic rocks with ages ranging from 3.36 to 2.69 Ga (Percival, 2007). Further subdivision of the Hudson Bay Terrane yields the Minto Block. The Minto Block underwent a major episode of igneous activity and crustal reworking from approximately 2.74 – 2.70 Ga (Milidragovic *et al.,* 2014). At this time, the proto-cratonic crust, largely composed of tonalite, trondhjemite, granodiorite (TTG) plutonic suites, underwent large-scale melting giving rise to voluminous granite, granodiorite, monzogranite (GGM) and pyroxene-bearing intermediate to felsic plutonic rocks (Milidragovic *et al.,* 2014).

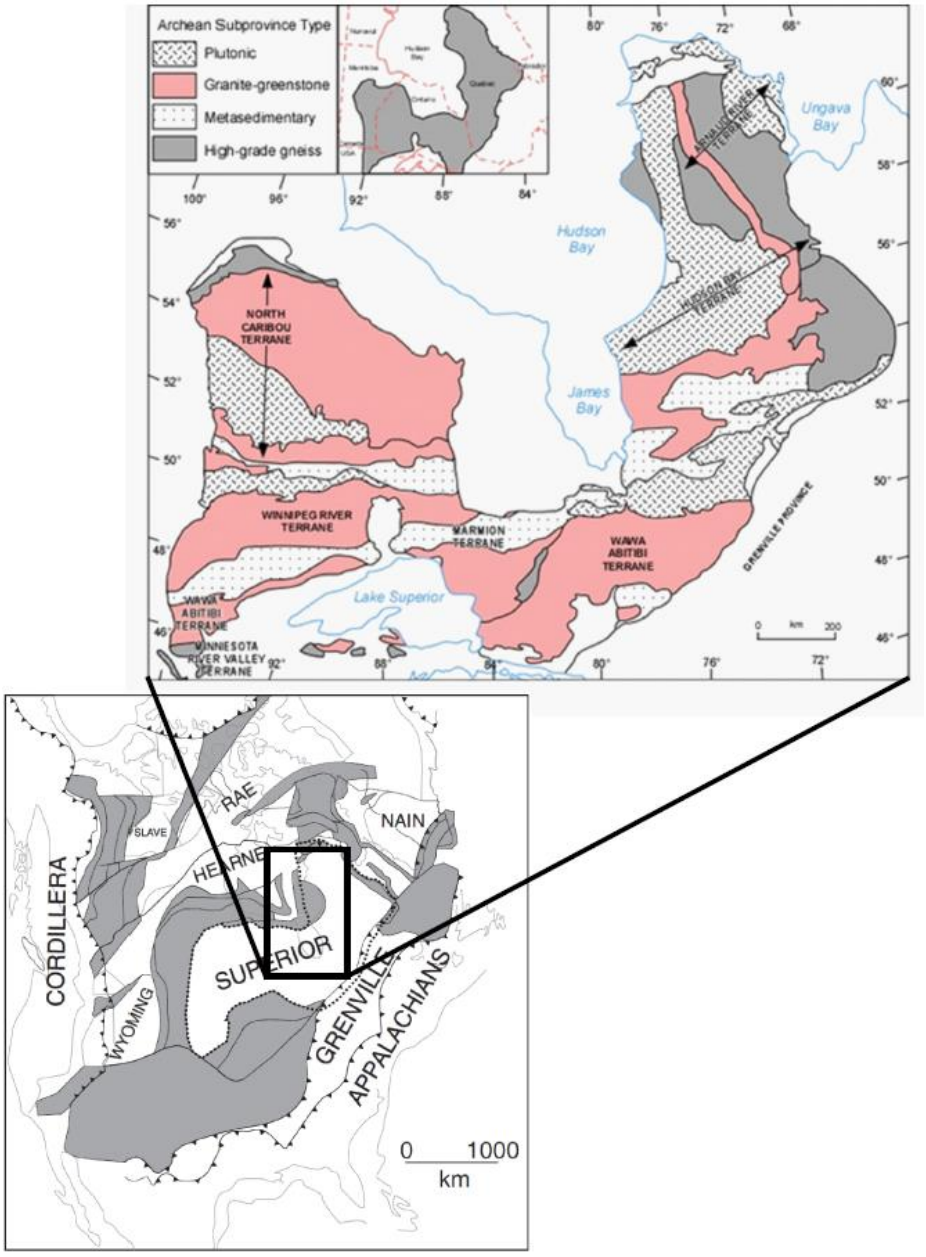

Figure 2.1: Major tectonic terrains of North America (Percival et al. 2012) with inset showing subprovince types of the Superior Province showing general locations of major terranes and rock types (modified from Card, 1990; Card and Paulsen, 1998).

CHAPTER III

RESEARCH DESIGN

METHODS

In total 70–120 cobble size clasts were collected from two sites each in the Decatur, Peoria, and Princeton sub-lobes, and one site in the Harvard sub lobe (Figure 3.1).

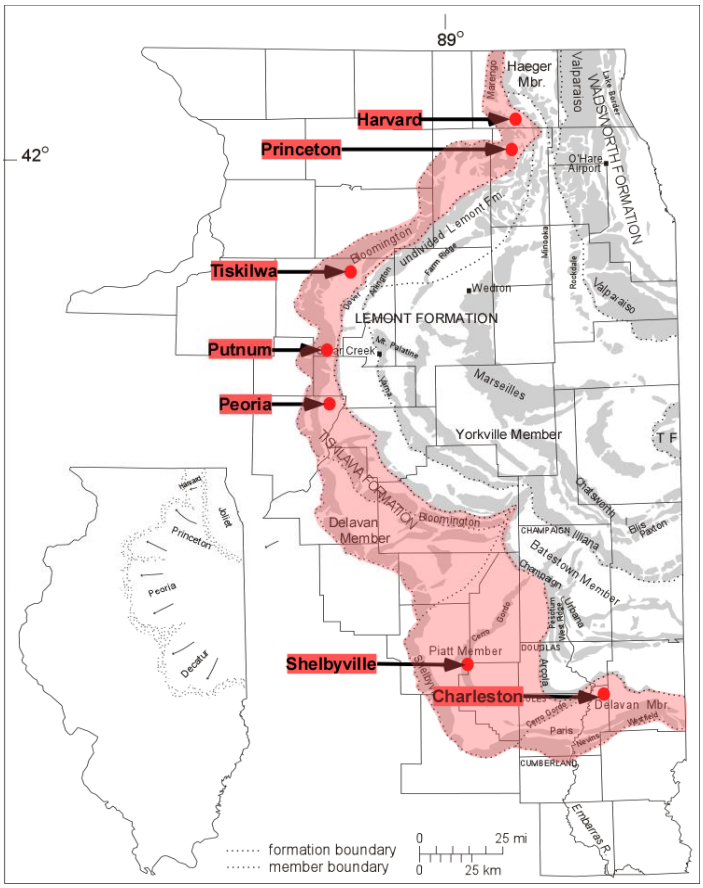

Figure 3.1: Map showing sampling locations. Red shading indicates Tiskilwa Till exposed at the surface (from Hansel and Johnson, 1996).

In total, 750 clasts were collected for sampling zircons. Only one sample was collected from the Harvard sub-lobe due to the smaller area in comparison to the other lobes. No samples were collected from the Joliet and Huron-Erie sublobes due to lack of outcrop and size of the lobe, respectively. The distribution of sites was determined on the accessibility of outcrops. Individual samples were photographed and the maximum diameter of each clast measured (Figures 3.2a, b).

Figure 3.2a: Total Clasts from one sample site

Figure 3.2b: Cobble-size clast

The general rock type of each clast was recorded and any non-crystalline rock clasts rejected (Table 1). The non-crystalline rocks were rejected to eliminate possible detrital zircons that were recycled from other sources. Each sample was crushed individually with a chipmunk crusher (Figure 3.3a) and then ground with a disc mill (Figure 3.3b).

TABLE 1: GENERAL ROCK TYPE FOR ALL SAMPLE LOCATIONS. (NOTE ONLEY CRYSALLINE ROCKS WERE USED FOR ANALYSIS).

Peoria		**Princeton**		**Putnum**	
Total Clasts	123	Total Clasts	107	Total Clasts	110
Tota Clasts Used	120	Tota Clasts Used	105	Tota Clasts Used	108
Granite	91	Granite	85	Granite	79
Granodiorite	21	Granodiorite	3	Granodiorite	13
Diorite	5	Diorite	17	Diorite	13
Rhyolite Porphry	3	Quartzite	2	Rhyolite Porphry	2
Carbonate	3			Quartzite	3
Shelbyville		**Harvard**		**Charleston**	
Total Clasts	95	Total Clasts	110	Total Clasts	108
Tota Clasts Used	93	Tota Clasts Used	105	Tota Clasts Used	108
Granite	62	Granite	93	Granite	71
Granodiorite	12	Granodiorite	8	Granodiorite	24
Diorite	17	Diorite	3	Diorite	11
Rhyolite	1	Quartize	5	Syenite	1
Carbonate	1	MonzoDiorite	1	Amphibolite Schist	1
Quartzite	1				
Amphibolite	1				
Tiskilwa		**All Sites**			
Total Clasts	97	Total	750		
Tota Clasts Used	95	Total Used	626		
Granite	52	Granite	533		
Granodiorite	16	Granodiorite	97		
Diorite	26	Diorite	92		
Rhyolite Porphry	1	Rhyolite Porpyry	6		
Carbonate	2	Rhyolite	1		
		Carbonate	6		
		Syenite	1		
		Amphibolite Schist	1		
		Amphibolite	1		
		MonzoDiorite	1		
		Quartzite	11		

Figure 3.3a: Chipmunk Crusher Figure 3.3b: Disk Mill

In order to avoid sampling bias, each sample was panned to a concentrate of heavy minerals (Figure 3.4a), dried, and one zircon selected from each concentrate using a binocular microscope (Figure 3.4b). When possible the first zircon viewed in the microscope aperture was selected for analysis.

Figure 3.4a: Panned Concentrate

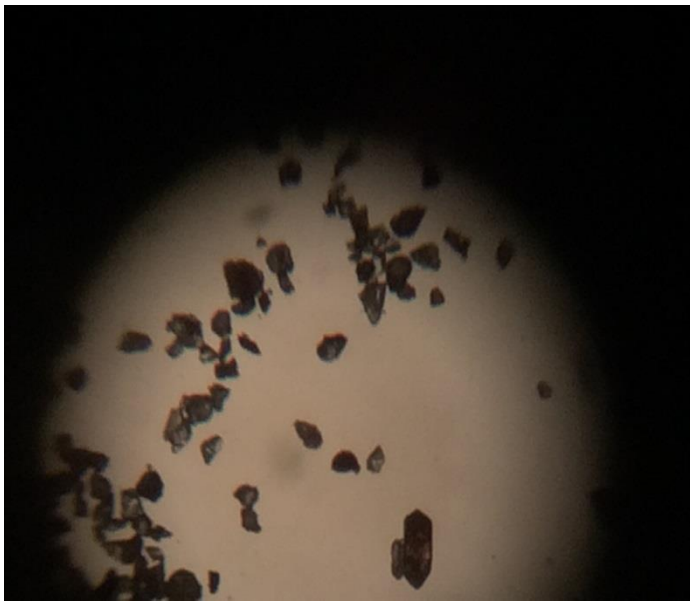

Figure 3.4b: Zircon in microscope view

Not only did this procedure counter bias, especially for samples that are more abundant in zircons, it also was more cost effective since heavy liquids and magnetic separation were not needed. Once the zircons were sampled, each sample site suite was placed into a vial and shipped to the University of Arizona Laserchron Center where they were mounted onto 1-inch diameter epoxy pucks along with fragments of three standards

The standards used are 1) Sri Lanka zircon, calibrated in-house by isotope dilution-thermal ionization (ID-TIMS) (Gehrels et al., 2008); 2) FC1 zircons from the Duluth Gabbro complex dated at 1099 ± 2 Ma (Paces and Miller, 1993; Schmitz et al., 2003); and 3) R33 zircon crystals yielding an age of 419.3 ± 0.4 Ma (Black et al., 2004).

These pucks were then polished to half thickness to expose the interior of the grains and cleaned. Cathodoluminescence (CL) images were taken for each mount to help in determining the location of laser pits and to identify zircon from other mineral grains (Figure 3.5).

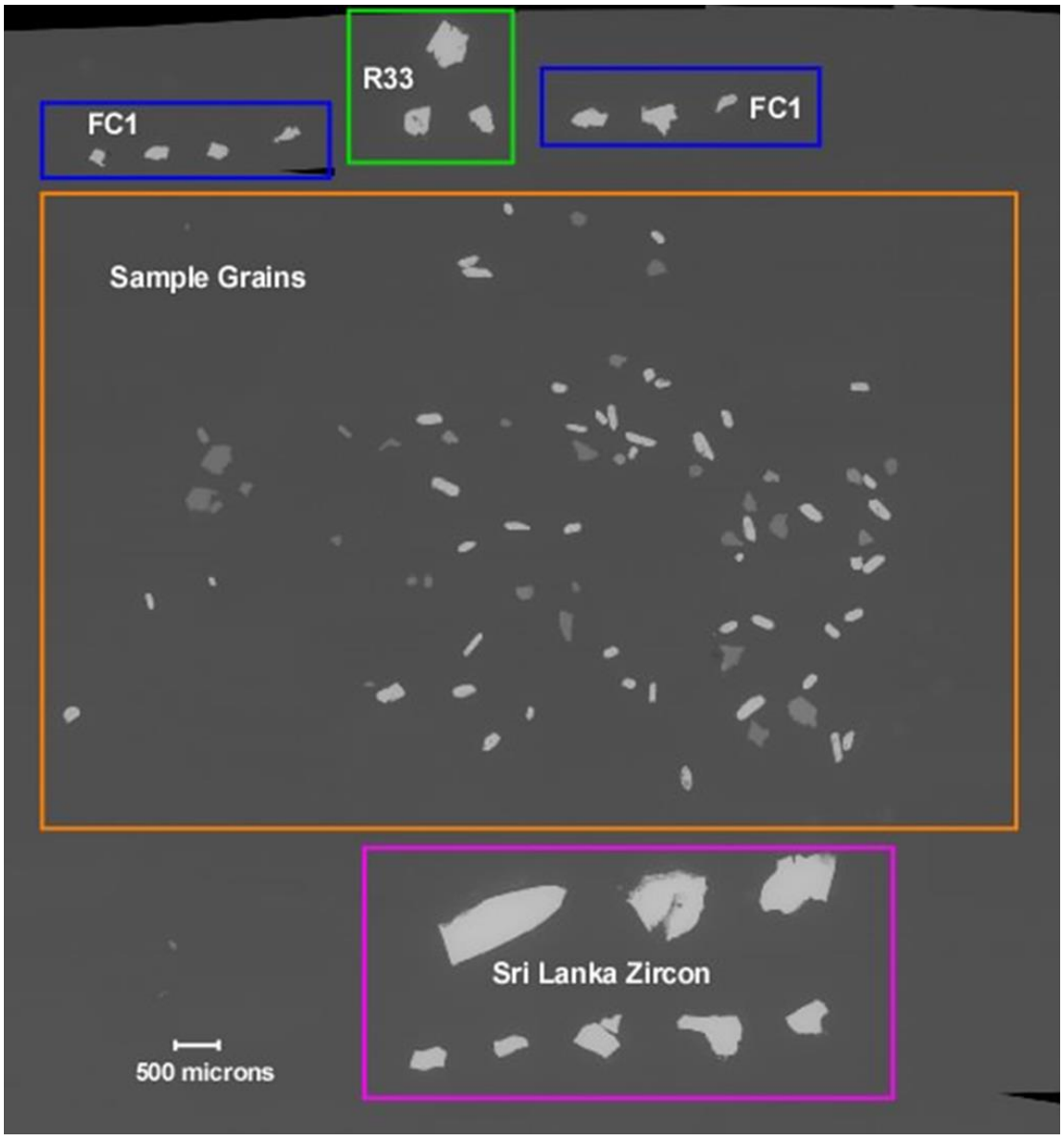

Figure 3.5: Mounted samples showing sample grains and the three standards used. The darker grains are impurities which were not analyzed.

U-Pb geochronology of zircons was conducted by laser ablation multicollector inductively coupled plasma mass spectrometry (LA-MC-ICPMS) at the Arizona LaserChron Center (Gehrels et al., 2008). The analyses involve ablation of zircon with a Photon Machines Analyte G2 Excimer laser using a spot diameter of 30 microns. The ablated material is carried in helium into the plasma source of a Nu HR ICPMS, which is equipped with a flight tube of sufficient width that U, Th, and Pb isotopes are measured simultaneously. All measurements are made in static mode, using Faraday detectors with $3x10^{11}$ ohm resistors for ^{238}U, ^{232}Th, ^{208}Pb-^{206}Pb, and discrete dynode ion counters for ^{204}Pb and ^{202}Hg. Ion yields are ~0.8 mv per ppm. Each analysis consists of one 15-second integration on peaks with the laser off (for backgrounds), 15 one-second integrations with the laser firing, and a 30 second delay to purge the previous sample and prepare for the next analysis. The ablation pit is ~15 microns in depth.

For each analysis, the errors in determining $^{206}Pb/^{238}U$ and $^{206}Pb/^{204}Pb$ result in a measurement error of ~1-2% (at 2-sigma level) in the $^{206}Pb/^{238}U$ age. The errors in measurement of $^{206}Pb/^{207}Pb$ and $^{206}Pb/^{204}Pb$ also result in ~1-2% (at 2-sigma level) uncertainty in age for grains that are >1.0 Ga, but are substantially larger for younger grains due to low intensity of the ^{207}Pb signal. For most analyses, the cross-over in precision of $^{206}Pb/^{238}U$ and $^{206}Pb/^{207}Pb$ ages occurs at ~1.0 Ga.

^{204}Hg interference with ^{204}Pb is accounted for measurement of ^{202}Hg during laser ablation and subtraction of ^{204}Hg according to the natural $^{202}Hg/^{204}Hg$ of 4.35. This Hg is correction is not significant for most analyses because our Hg backgrounds are low (generally ~150 cps at mass 204).

Common Pb correction is accomplished by using the Hg-corrected ^{204}Pb and assuming an initial Pb composition from Stacey and Kramers (1975). Uncertainties of 1.5 for ^{206}Pb/^{204}Pb and 0.3 for ^{207}Pb/^{204}Pb are applied to these compositional values based on the variation in Pb isotopic composition in modern crystal rocks.

Inter-element fractionation of Pb/U is generally ~5%, whereas apparent fractionation of Pb isotopes is generally <0.2%. In-run analysis of fragments of a large zircon crystal (generally every fifth measurement) with known age of 563.5 ± 3.2 Ma (2-sigma error) is used to correct for this fractionation. The uncertainty resulting from the calibration correction is generally 1-2% (2-sigma) for both ^{206}Pb/^{207}Pb and ^{206}Pb/^{238}U ages. Concentrations of U and Th are calibrated relative to our Sri Lanka zircon, which contains ~518 ppm of U and 68 ppm Th.

The analytical data are reported in Appendix C. Uncertainties shown in these tables are at the 1-sigma level, and include only measurement errors. Analyses that are >20% discordant (by comparison of ^{206}Pb/^{238}U and ^{206}Pb/^{207}Pb ages) or >5% reverse discordant are not considered further.

The resulting interpreted ages are shown on Pb*/U concordia diagrams and weighted mean diagrams using the routines in Isoplot (Ludwig, 2008). The weighted mean diagrams show the weighted mean (weighting according to the square of the internal uncertainties), the uncertainty of the weighted mean, the external (systematic) uncertainty that corresponds to the ages used, the final uncertainty of the age (determined by quadratic addition of the weighted mean and external uncertainties), and the MSWD of the data set.

The data reduction was completed using a fully automated Excel spreadsheet and data imported from Isoprobe files (Gehrels et al, 2008). All corrections and calculations were performed in the database, including ages, uncertainties, and error correlations. Analyses that were >10% discordant or >5% reversely discordant were excluded. The "best ages" (those with the smallest error of the three ages generated) were used to determine crystallization ages of the zircons, and relative probability density plots were constructed with these ages using Isoplot (Ludwig, 2008). The ages acquired by the LA-MC-ICPMS data was compared to up-ice bedrock crystallization ages determined by Card (1990), Percival and Easton (2007), Lasalle *et. al*. (2014) and Raharimahefa *et. al.* (2014).

CHAPTER IV

ANALYSIS OF THE DATA

RESULTS

In total 301 zircons were analyzed for the study. Zircons that were >10% discordant and >5% reverse discordant were not used in the data analysis. The sample population is dominated by Archean (2.5 – 3 Ga) age zircons with the peak age being 2703 Ma. Concordia diagrams were also constructed for the samples, all showing similar Concordia ages. All detailed zircon geochronology data are found in Appendix C. A Kolmogorov-Smirnov (K-S) test was also applied to the data comparing the groups to one another. The K-S compares two or more distributions of data to determine if there is any significant difference between populations. The probability (P) value generated by the K-S test indicates the likelihood of the samples coming from different populations. The higher the P value the less likely the populations came from different sources. The level of confidence is set at 95%. While the K-S test cannot distinguish if the populations are the same, it can show if the samples are from the same parent location (Gehrels, 2012). The K-S test showed no significant difference between samples indicating that it is statistically likely that the till was generated from the same source area (Table 1).

TABLE 2: K-S VALUES WITH ERROR

	Peoria	Harvard	Tiskilwa	Putnam	Genoa	Shelbyville	Charleston
Peoria		1.000	0.634	0.763	1.000	0.997	0.326
Harvard	1.000		0.955	0.966	1.000	1.000	0.352
Tiskilwa	0.634	0.955		1.000	0.887	0.454	0.982
Putnam	0.763	0.966	1.000		0.909	0.593	0.997
Genoa	1.000	1.000	0.887	0.909		0.999	0.374
Shelbyville	0.997	1.000	0.454	0.593	0.999		0.220
Charleston	0.326	0.352	0.982	0.997	0.374	0.220	

Cumulative probability (Figure 4.1) and frequency plots (Figure 4.2) were also prepared with the data, both showing the remarkable lack of variability within the data set with both having peak ages at 2703 Ma.

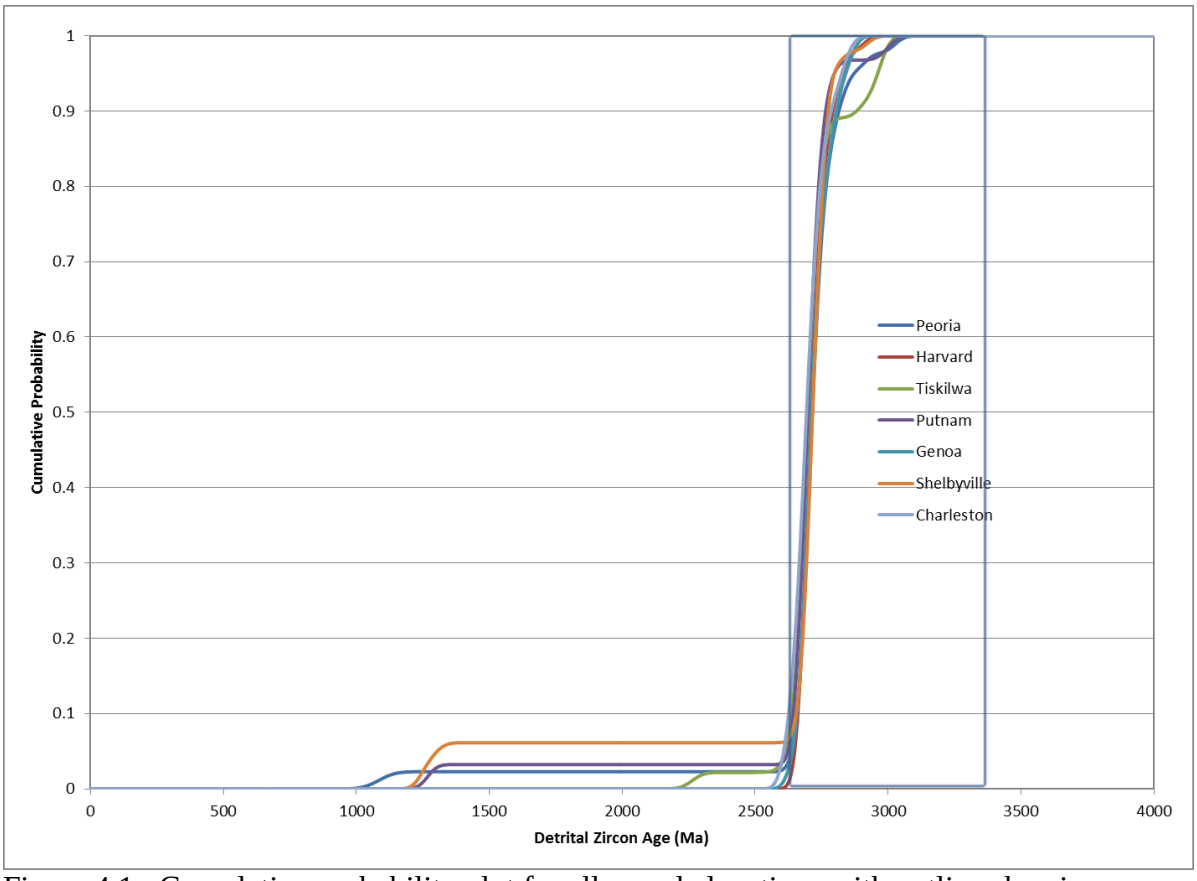

Figure 4.1: Cumulative probability plot for all sample locations with outline showing age range of Hudson Bay Terrane (3.36 – 2.69 Ga).

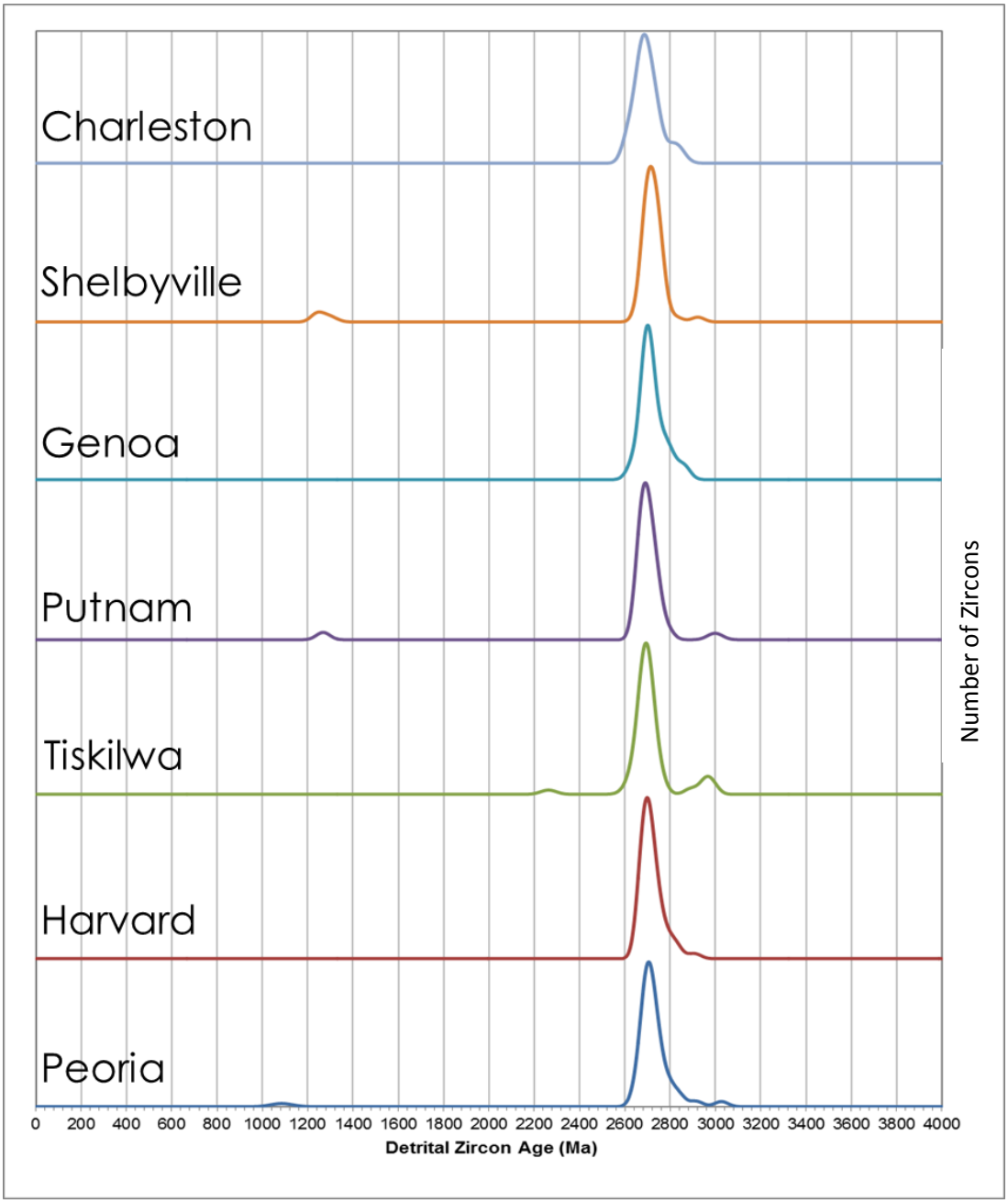

Figure 4.2: Frequency plots of all sample locations.

DISCUSSION

The dominance of Archean age grains in all of the samples is noteworthy. With all the samples combined showing a peak age of 2703 Ma, the source area for the Tiskilwa till is most certainly derived from the Superior Province and specifically from the Minto Block (Figure 2.1).

Perhaps as important is the similarity of results between this study and a more localized study on the Bloomington and Normal Moraines performed by Rickels (2016). Rickels performed the same geochronology methods and collected clasts locally from the Tiskilwa till and the Batestown member of the Lemont formation (Figure 1.1) (Rickels, 2016). Both locations sampled by Rickels were on a recessional moraine as opposed to the terminal moraines sampled in this study. Rickels' data show peak ages of 2.774 Ga and 2.747 Ga indicating that the provenance of both studies are similar (2016).

This study reaffirms earlier work stating that the ice flow had a Lake Michigan lobe source. If more than one source area was incorporated within the ice, the clast data would have shown more diversity in age. With the data showing such a distinct peak in age, the data supports earlier work that established the ice flow in Illinois as having a Lake Michigan lobe source.

The data and techniques used in this study could potentially be used to support ice flow dynamics. For example, work done by Dyke and Prest (1987) shows the Laurentide ice sheet having several main domes (Figure 4.3). With the lack in variability of clasts, the data collected in this study could support the location of the Hudson Bay dome as the majority of the clasts were likely derived from the Hudson Bay region.

Further studies would be needed along the ice margins to potentially confirm the existence, or lack thereof, of other domes.

While the data does not lead to revisions of ice flow in Illinois, it does give rise to some questions. One such question is that can the data be used to show system consistencies? The lack of variability in the data collected could show consistencies of the Laurentide sheet. Another question that could potentially be solved using this method is, why is the Tiskilwa Formation till so thick when we do not see modern glaciers depositing such thick tills? Perhaps till geochronology on cobbles could be utilized to determine rates of deposition. Lastly, perhaps the method of only sampling cobbles could grant insights into how ice stream dynamics work in current glaciers.

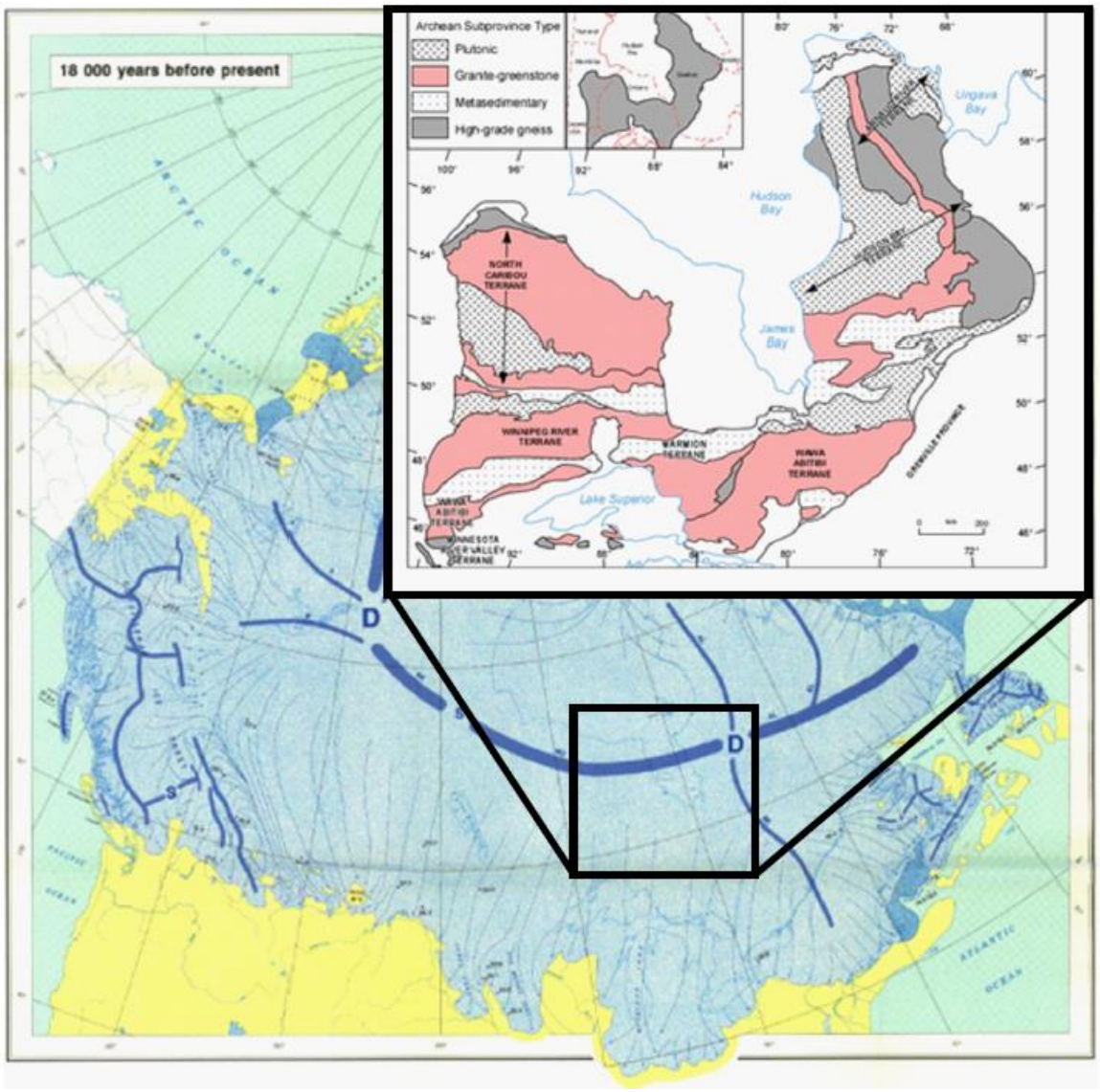

Figure 4.3: Laurentide ice sheet reconstruction showing ice domes from Dyke and Prest, (1987). Inset showing Superior Province from Card and Paulsen (1998).

CHAPTER V

SUMMARY, CONCLUSIONS, AND RECOMMENDATIONS

CONCLUSION

The initial hypothesis that U/Pb dating on glacial erratics in the Tiskilwa Formation till could lead to a revision in glacial lobes of the Wisconsinan episode was not supported. While the data collected during this study did not support the initial hypothesis; however, the data did lead to some important insights on the geochronology of cobbles in glacial till. Geochronology on the Tiskilwa till confirms work performed by Johnson *et al.* (2006) indicating the source area for the till being derived from one Lake Michigan Lobe. The hypothesis that U-Pb ages collected from clasts could lead to a refinement in source area was supported. Zircon analyses further refined the source area to the Hudson Bay Terrain of the Superior Province.

In comparing this studies results, the data collected correlated with data collected by Rickels (2016) on more localized tills. This could prove to be useful as it demonstrated that both regionally and locally, the Tiskilwa till likely has the same provenance. This also demonstrates that the terminal and recessional moraines maintained the same source area.

While the hypothesis that U-Pb geochronology could lead to a revision of the Wisconsinan age sub-lobes was not supported, the study was successful in using U-Pb geochronology of crystalline cobbles to determine provenance. Further studies are needed to determine if geochronology of cobbles could lead to glacial lobe revision or perhaps further insights on ice flow dynamics. Further studies are also needed to determine it the methodology of selecting only one zircon from each clast could prove to be useful in other till provenance.

REFERENCES

Averill S.A. 2001. The application of heavy indicator minerals in mineral exploration. In: McClenaghan M.B., Bobrowsky P.T., Hall G.E.M., Cook S. (eds) Drift Exploration in Glaciated Terrain. Geological Society of London, Special Volume, 185, 69–82.

Black, L., Kamo, S., Allen, C., Davis, D., Aleinikoff, J., Valley, J., Mundil, R., Campbell, I., Korsch, R., Williams, I., and Foudoulis, C., 2004, Improved 206Pb/238U microprobe geochronology by the monitoring of a trace-element-related matrix effect; SHRIMP, ID–TIMS, ELA–ICP–MS and oxygen isotope documentation for a series of zircon standards: Chemical Geology, v. 205, p. 115-140.

Card, K. D., & Ciesielski, A., 1986, DNAG# 1. Subdivisions of the Superior Province of the Canadian shield. *Geoscience Canada*, v. *13*, n. 1

Card, K.D. and Paulsen, K.H., 1998, Geology and mineral deposits of the Superior Province of the Canadian Shield, Chapter 2, in Geology of the Precambrian Superior and Grenville Provinces and Precambrian Fossils in North America: Geological Survey of Canada, Geology of Canada Series no. 7, p.13-204.

Card, K.D., 1990, A Review of the Superior Province of the Canadian Shield, a product of Archean accretion. Precambrian Res., 48: 99-156.

Chamberlin, T.C., 1878, On the extent and significance of the Wisconsin kettle moraine: Wisconsin Academy of Science Transactions, v. 4, p. 201-234.

Curry, B.B., D.A. Grimley, and E.D. McKay III, 2011, Quaternary glaciations in Illinois (Chapter 37), in J. Ehlers, P.L. Gibbard and P.D. Hughes, eds., Developments in Quaternary Science, v. 15, Amsterdam, The Netherlands, Elsevier, p. 467–487.

Dreimanis A., Vagners U., 1971. Till: A Symposium Bimodal distribution of rock and mineral fragments in basal tills, ed Goldthwait R. P. (Ohio State University Press), p 237–250.

Doornbos, C., Heaman, L M., Doupe, J. P., England, J., Simonetti, A., Lajeunesse, P., 2009, The first integrated use of in situ U–Pb geochronology and geochemical analyses to determine long-distance transport of glacial erratics from mainland Canada into the western Arctic Archipelago: Canadian Journal of Earth Science, v. 46, p. 101-122.

Dyke, A. S., & Prest, V. K., 1987. Late Wisconsinan and Holocene history of the Laurentide ice sheet. *Géographie physique et Quaternaire*, v. *41*, n. 2, 237-263.

Gehrels, G., 2012. Detrital zircon UePb geochronology: current methods and new opportunities. In: Busby, C., Azor, A. (Eds.), Tectonics of Sedimentary Basins: Recent Advances. Blackwell Publishing, pp. 47e62.

Gehrels, G.E., Valencia, V., Ruiz, J., 2008, Enhanced precision, accuracy, efficiency, and spatial resolution of U-Pb ages by laser ablation–multicollector–inductively coupled plasma–mass spectrometry: Geochemistry, Geophysics, Geosystems, v. 9, p. 19-37.

Gwyn. Q.H.J., and A. Dreimanis, 1979, Heavy mineral assemblages in tills and their use in distinguishing glacial lobes in the Great Lakes region: Canadian Journal of Earth Sciences, v. 16, p. 2219–2235.

Hansel, A.K., and Johnson, W.H., 1996, Wedron and Mason Groups: Lithostratigraphic Reclassification of Deposits of the Wisconsin Episode, Lake Michigan Lobe Area: Illinois State Geological Survey, Bulletin 104

Hansel, A.K., and Johnson, W.H., 1992, Fluctuations of the Lake Michigan Lobe during the late Wisconsin Subepisode: Sveriges Geologiska Undersökning, Series Ca 81, p. 133-144.

Johnson, W. H., Hansel, A. K., 1990, Multiple Wisconsinan Glacigenic Sequences At Wedron, Illinois: Journal of Sedimentary Petrology, v. 60, n 1, p. 26-41.

Johnson, W. H., Moore, D.W., and McKay, E.D., 1986, Provenance of late Wisconsinan (Woodfordian) till and origin of the Decatur sublobe, east-central Illinois: Geological Society of America Bulletin, v. 97, p. 109 8–11.

Lasalle, S., Dunning, G., Indares, A., 2014, In situ LA–ICP–MS dating of monazite from aluminous gneisses: insights on the tectono-metamorphic history of a granulite-facies domain in the central Grenville Province: Canadian Journal of Earth Science, v. 51, p. 558-572.

Leverett, F and Taylor, F.B., 1915, The Pleistocene of Indiana and Michigan and the History of the Great Lakes: U.S. Geological Survey Monograph 53, 529 p.

Licht, K. J., and E. F. Palmer (2013), Erosion and transport by Byrd Glacier, Antarctica during the Last Glacial Maximum, Quat. Sci. Rev., 62, 32–48, doi:10.1016/j.quascirev.2012.11.017.

Lusardi, B. A., Jennings, C. E., and Harris, K. L., 2011, Provenance of Des Moines lobe till records ice stream catchment evolution during Laurentide deglaciation: Boreas, v. 40, p. 585 – 597.

Ludwig, R.K., 2008, Isoplot 3.6: Berkeley Geochronology Center, Special Publication 4, 77 p.

Malone, D.H., Craddock, J.P., and Mathesin, M.K., 2014, Age and Provenance of Allochthonous Volcanic Rocks at Squaw Peaks, WY: Implications for the Heart Mountain Slide: The Mountain Geologist, v. 51, n. 4, p. 229-344.

Malone, D.H., Craddock, J.P., and Schroeder, K.A., 2014, Detrital Zircon Age and Provenance of Wapiti Formation (Eocene) Tuffaceous Sandstones, South Fork Shoshone River Valley, Wyoming: The Mountain Geologist, v. 51, n. 4, p. 271-286.

Milidragovic, D., Francis, D., Weis, D., & Constantin, M., 2014, Neoarchean (c. 2· 7 Ga) Plutons of the Ungava Craton, Québec, Canada: Parental Magma Compositions and Implications for Fe-rich Mantle Source Regions.*Journal of Petrology*, v. *55*, n. 12, p. 2481-2512.

McClenaghan, M. B., Thorleifson, L. H., and DiLabio, R. N. W., 2000, Till geochemical and indicator mineral methods in mineral exploration. *Ore Geology Reviews*, *16*(3), 145-166.

Paces, J.B., and Miller, J.D., 1993, Precise U-Pb ages of Duluth Complex and related mafic intrusions, northeastern Minnesota: Geochronological insights to physical, petrogenetic, paleomagnetic, and tectonomagmatic processes associated with the 1.1 Ga midcontinent rift system: Journal of Geophysical Research, v. 98, p. 13997-14013.

Percival, J.A. and Easton, R.M. 2007. Geology of the Canadian Shield in Ontario: an update; Ontario Geological Survey, Open File Report 6196, Geological Survey of Canada, Open File 5511, Ontario Power Generation, Report 06819-REP-01200-10158-R00, 65p.

Percival, J.A., Skulski, T., Sanborn-Barrie, M., Stott, G.M., Leclair, A.D., Corkery, M.T., and Boily, M. 2012, Geology and tectonic evolution of the Superior Province, Canada. Chapter 6 *In* Tectonic Styles in Canada: The LITHOPROBE Perspective. *Edited by* J.A. Percival, F.A. Cook, and R.M. Clowes. Geological Association of Canada, Special Paper 49, pp. 321–378.

Prest, V. K., Donaldson, A., Mooers, H. D., 2000, The Omar Story: The Role of Omars in Assessing Glacial History of West-Central North America: Geographie physique et Quaternaire, v. 54, n.3, p. 257-270.

Plouffe, A, Bednarski, J.M., Huscroft, C.A., Anderson, R.G., and McCuaig, S.J., 2011, Late Wisconsinan glacial history in the Bonaparte Lake map area, south-central British Columbia: implications for glacial transport and mineral exploration: Canadian Journal of Earth Sciences, v. 48, p. 1091-1111.

Raharimahefa, T., Lafrance, B., Tinkham, D. K., 2014, New structural, metamorphic, and U–Pb geochronological constraints on the Blezardian Orogeny and Yavapai Orogeny in the Southern Province, Sudbury, Canada: Canadian Journal of Earth Science, v. 51, p. 750-774.

Rickels, E.S., 2016, Surficial Geology and Provenance of Glacial Deposits of the Saybrook 7.5 Minute Quadrangle, McLean County, Illinois. [M.S. Thesis] Illinois State University, 53p

Roy, M., Clark, P.U., Duncan, R.A. and Hemming, S.R. 2007, Insights into the late Cenozoic configuration of the Laurentide Ice Sheet from 40Ar/39Ar dating of glacially transported minerals in midcontinent tills, Geochemistry Geophysics Geosystems, 8: 1-12.

Schmitz, M.D., Bowring, S.A., and Ireland, T., 2003, Evaluation of Duluth Complex anorthositic series (AS3) zircon as a U-Pb geochronological standard: New high-precision isotope dilution thermal ionization mass spectrometry results: Geochimica et Cosmochimica Acta, v. 67, n. 19, p. 3665-3672.

Stacey, J.S., and Kramers, J.D., 1975, Approximation of terrestrial lead isotope evolution by a two-stage model: Earth and Planetary Science Letters, v. 26, p. 207-221.

Wickham, S. S., Johnson, W. H., Glass, H. D., 1988. Regional Geology of T he Tiskilwa Till Member, Wedron Formation, Northeastern Illinois: Illinois State Geological Survey. Circular, 543.

Welke, B., Licht, K., Hennessy, A., Hemming, S., Pierce Davis, E., & Kassab, C., 2016. Applications of detrital geochronology and thermochronology from glacial deposits to the Paleozoic and Mesozoic thermal history of the Ross Embayment, Antarctica. *Geochemistry, Geophysics, Geosystems*, v. *17*, n. 7, p. 2762-2780.

Willman, H.B., and J.C. Frye, 1970, Pleistocene stratigraphy of Illinois: Illinois State Geological Survey, Bulletin 94, 204 p.

Zimmermann, U., Andersen, T., Madland, M. V., & Larsen, I. S., 2015, The role of U-Pb ages of detrital zircons in sedimentology—An alarming case study for the impact of sampling for provenance interpretation. *Sedimentary Geology*, v. *320*, p. 38-50.

APPENDIX A

FREQUENCY PLOTS FOR ALL SAMPLING LOCATIONS

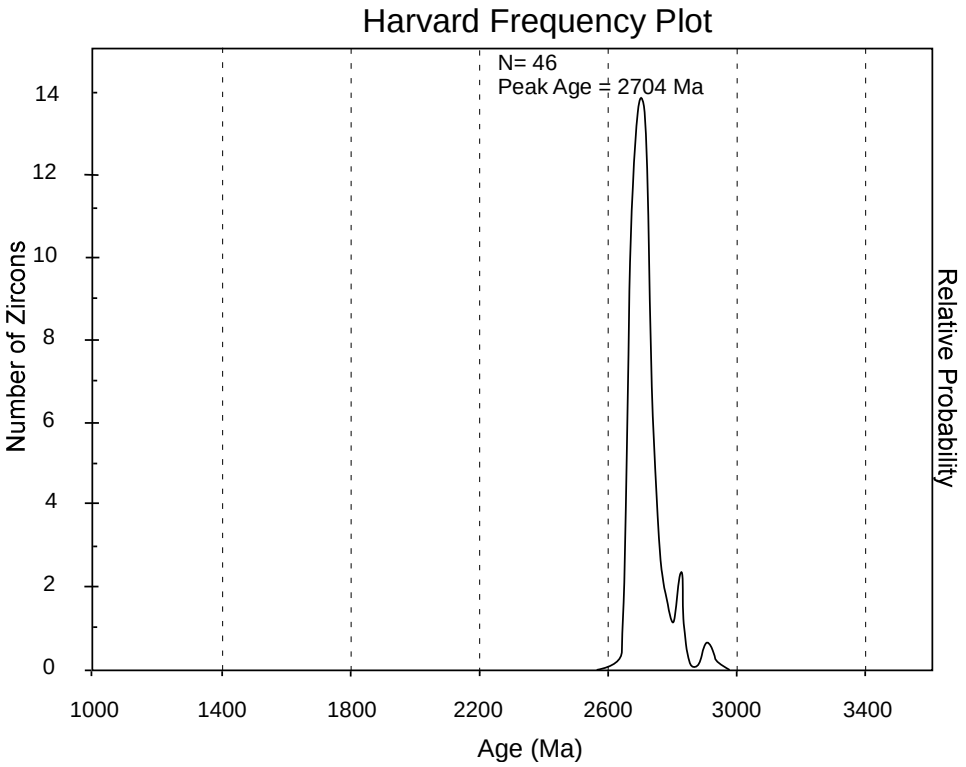

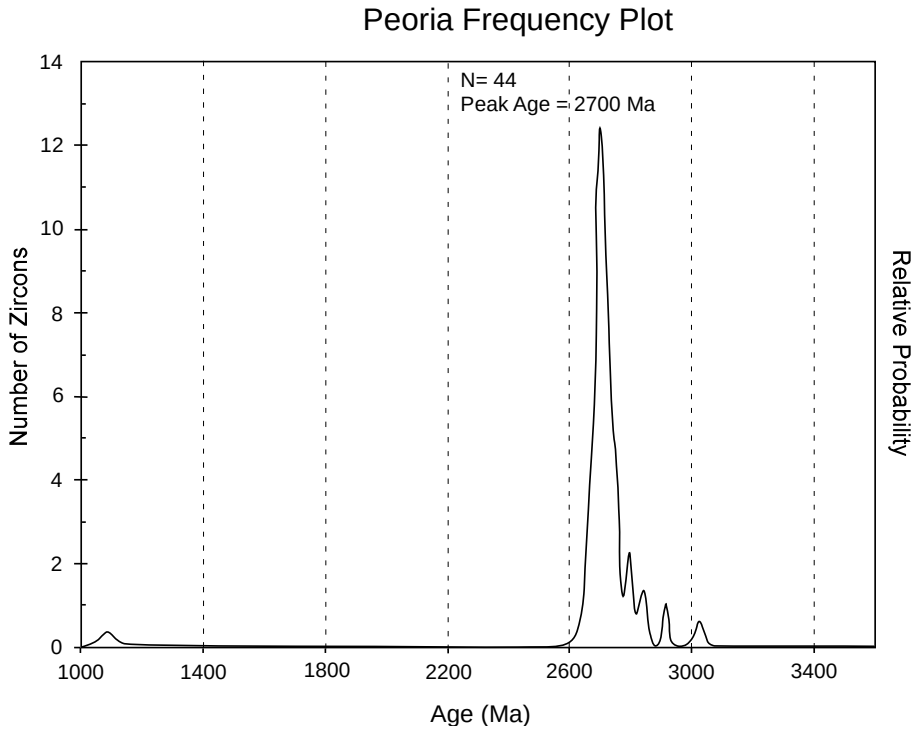
Peoria Frequency Plot
N= 44
Peak Age = 2700 Ma
Number of Zircons
Relative Probability
Age (Ma)
0
2
4
6
8
10
12
14
1000
1400
1800
2200
2600
3000
3400

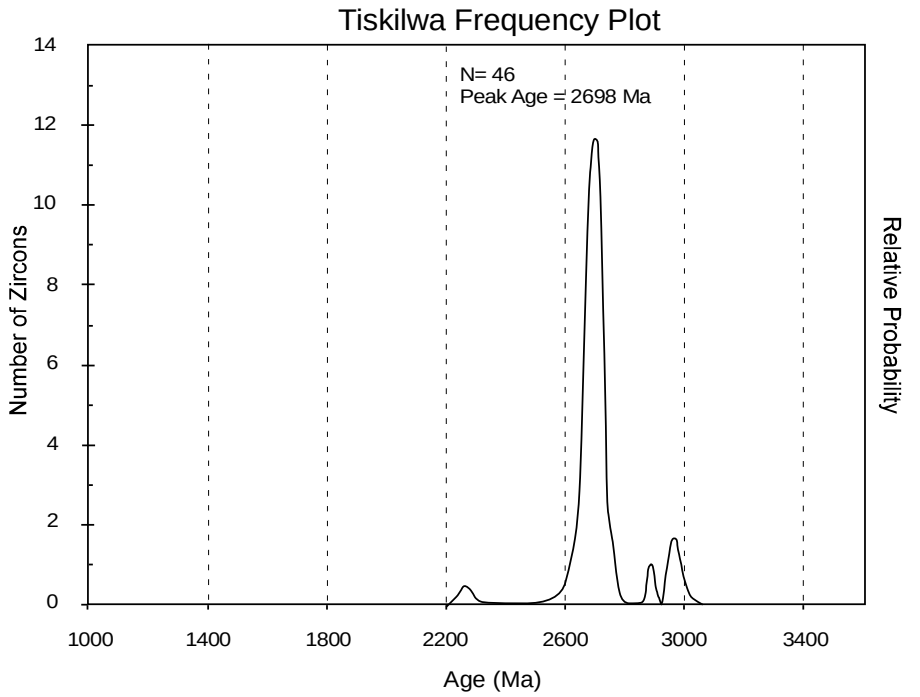
Tiskilwa Frequency Plot
N= 46
Peak Age = 2698 Ma
Number of Zircons
Relative Probability
Age (Ma)
0
2
4
6
8
10
12
14
1000
1400
1800
2200
2600
3000
3400

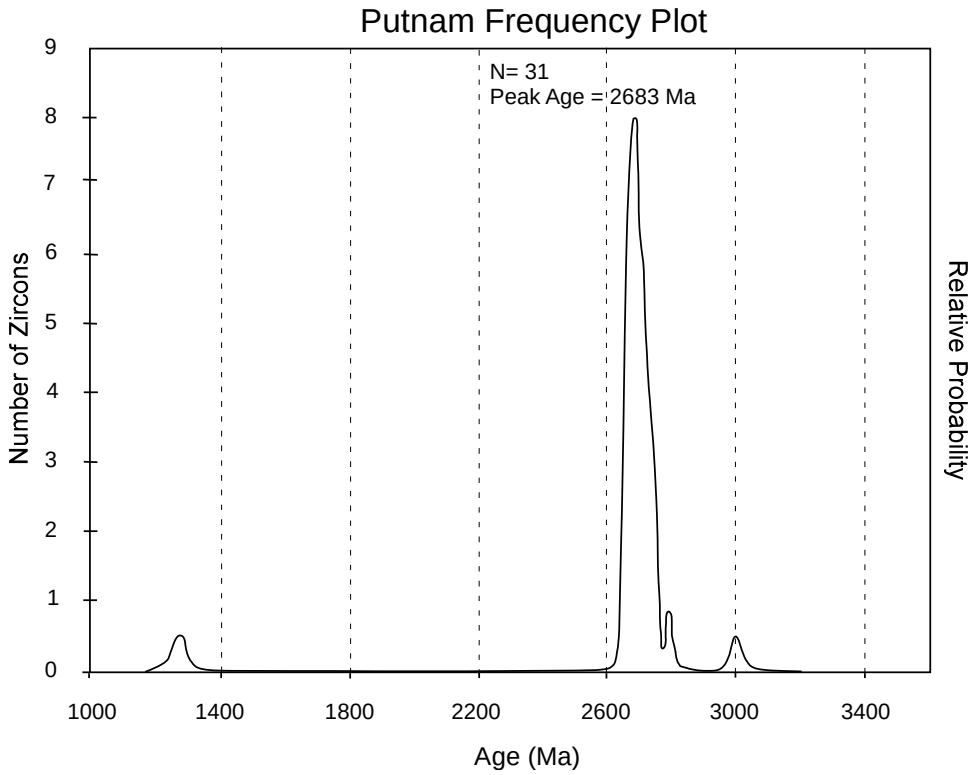
Putnam Frequency Plot
N= 31
Peak Age = 2683 Ma
Number of Zircons
Relative Probability
Age (Ma)
0
1
2
3
4
5
6
7
8
9
1000
1400
1800
2200
2600
3000
3400

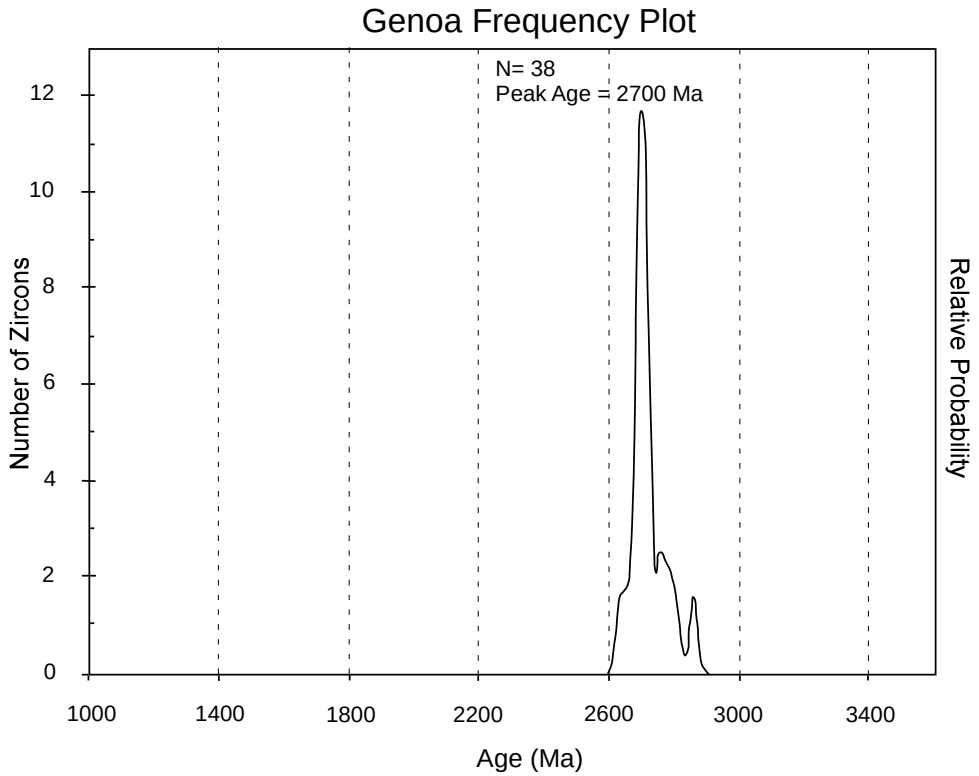
Genoa Frequency Plot
N= 38
Peak Age = 2700 Ma
Number of Zircons
Relative Probability
Age (Ma)
0
2
4
6
8
10
12
1000
1400
1800
2200
2600
3000
3400

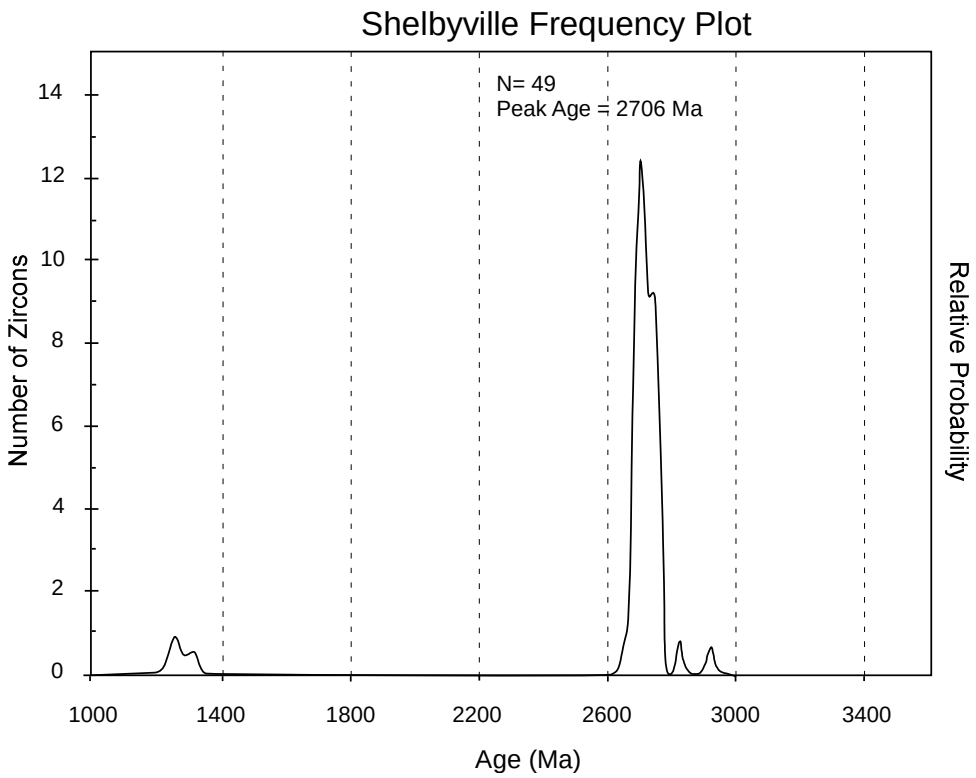
Shelbyville Frequency Plot
N= 49
Peak Age = 2706 Ma
Number of Zircons
Relative Probability
0
2
4
6
8
10
12
14
1000
1400
1800
2200
2600
3000
3400
Age (Ma)

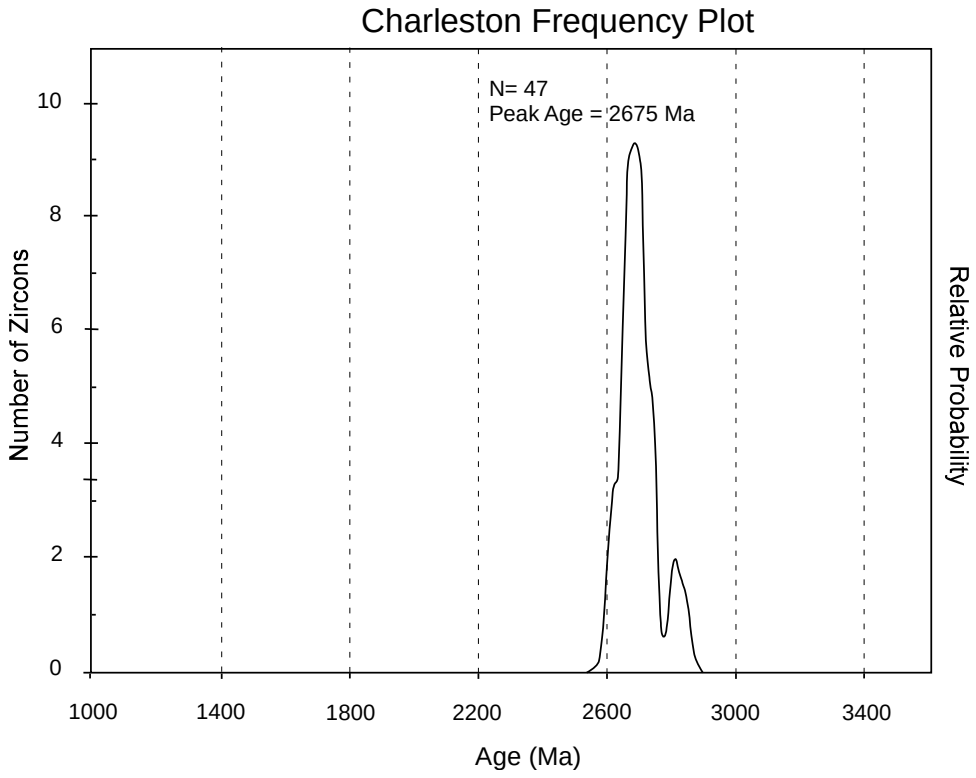
Charleston Frequency Plot
N= 47
Peak Age = 2675 Ma
Number of Zircons
Relative Probability
0
2
4
6
8
10
1000
1400
1800
2200
2600
3000
3400
Age (Ma)

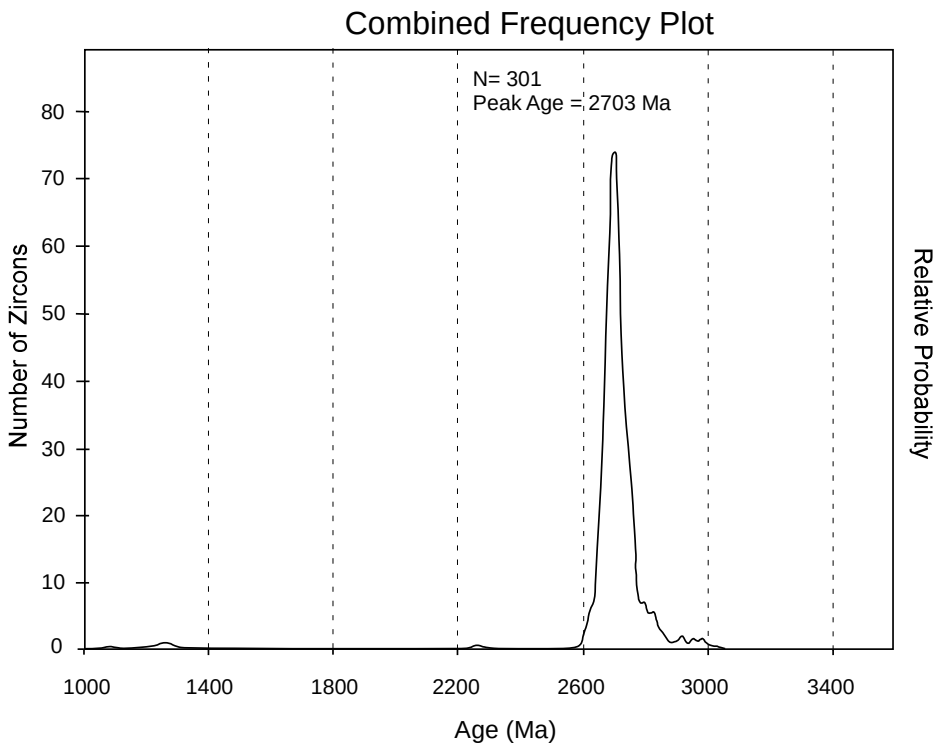
Combined Frequency Plot
N= 301
Peak Age = 2703 Ma
Number of Zircons
Relative Probability
0
10
20
30
40
50
60
70
80
1000
1400
1800
2200
2600
3000
3400
Age (Ma)

APPENDIX B

CONCORDIA PLOTS FOR ALL SAMPLING LOCATIONS

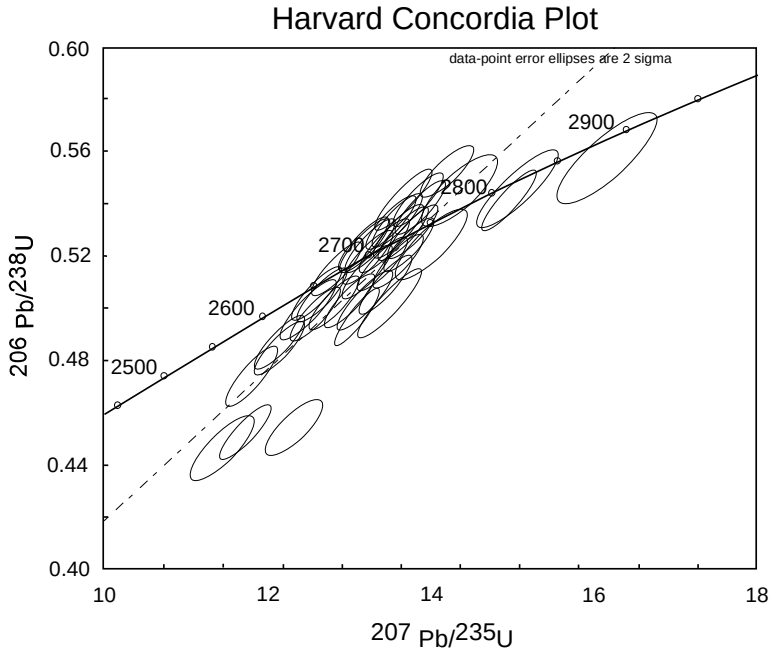

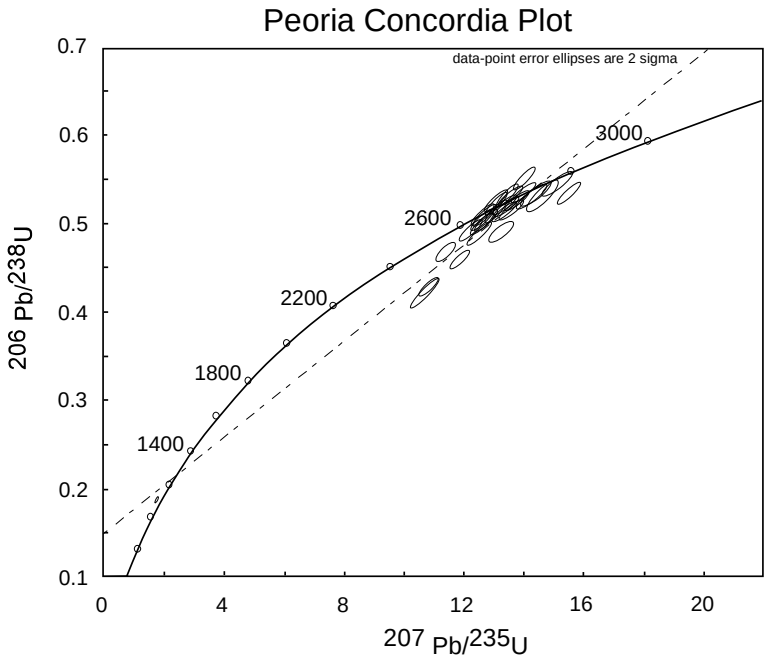
Peoria Concordia Plot
data-point error ellipses are 2 sigma
0.7
0.6
0.5
0.4
0.3
0.2
0.1
206 Pb/238U
0
4
8
12
16
20
207 Pb/235U
3000
2600
2200
1800
1400

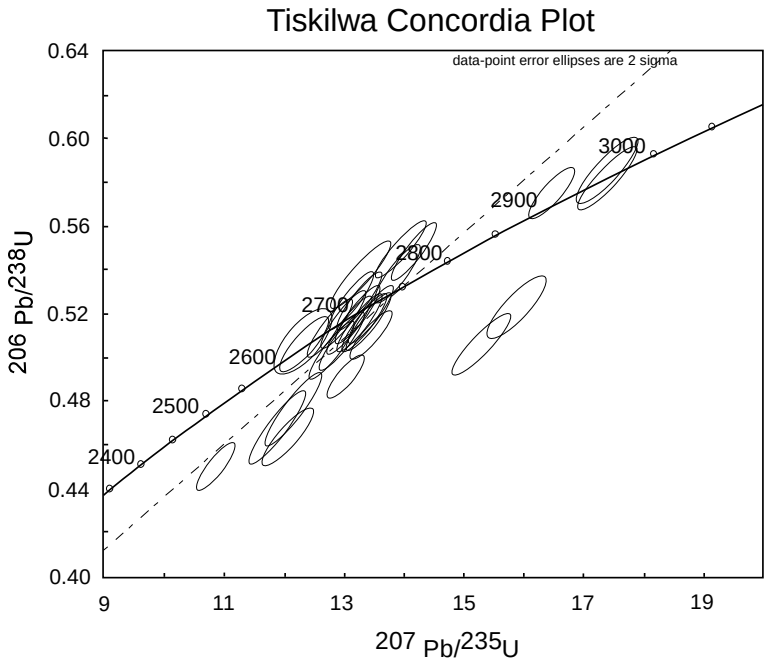
Tiskilwa Concordia Plot
data-point error ellipses are 2 sigma
0.64
0.60
0.56
0.52
0.48
0.44
0.40
206 Pb/238U
9
11
13
15
17
19
207 Pb/235U
3000
2900
2800
2700
2600
2500
2400

Putnam Concordia Plot

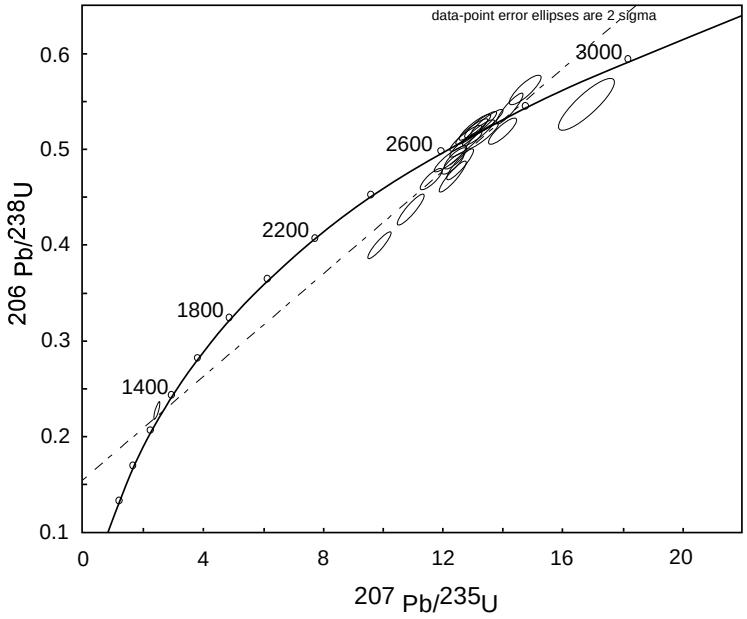

Genoa Concordia Plot

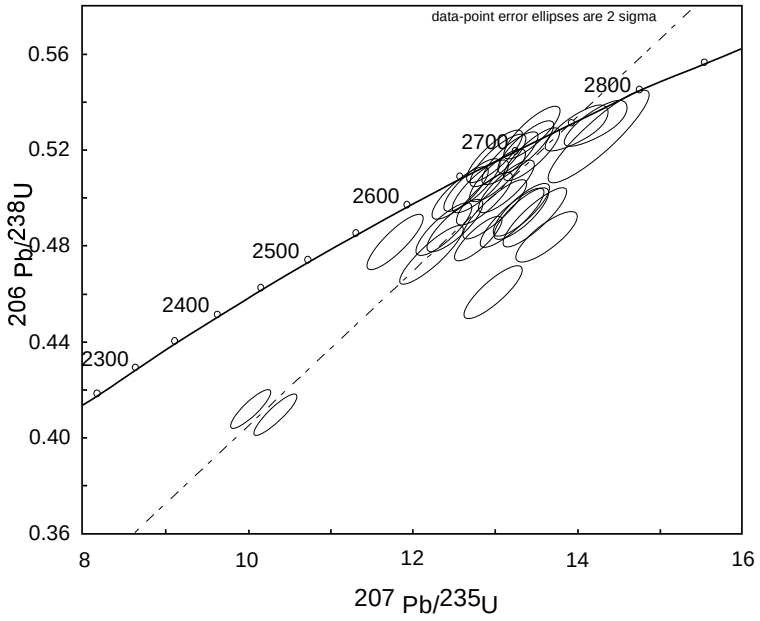

Shelybville Concordia Plot

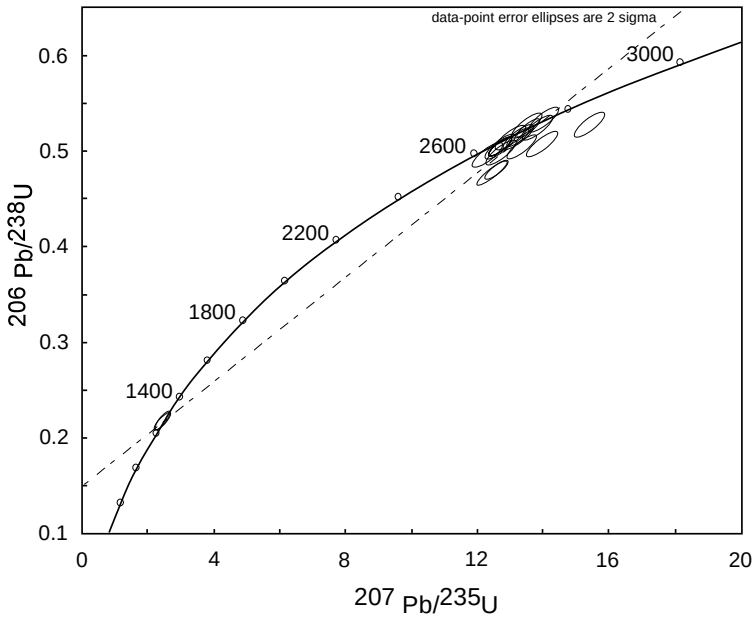

Charleston Concordia Plot

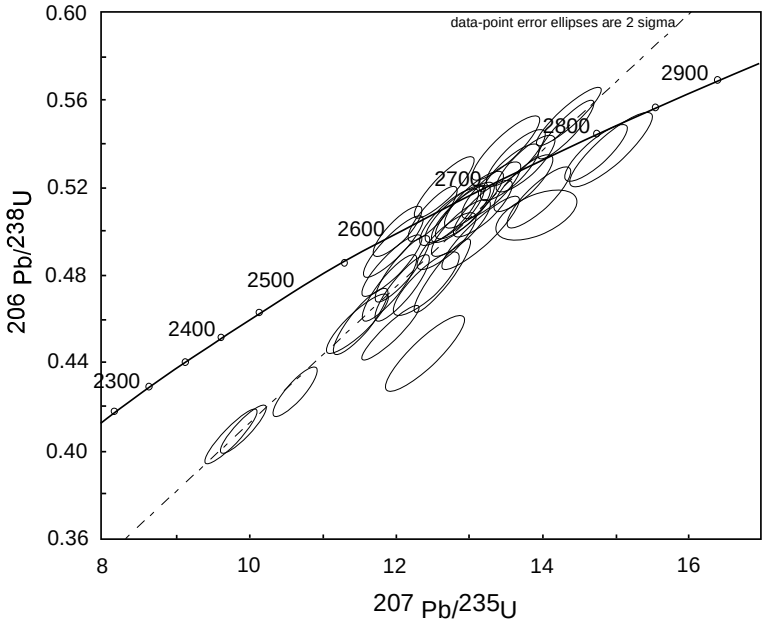

APPENDIX C

COMPLETE DATA FOR ALL SAMPLING LOCATIONS

1. 1. Analyses with >10% uncertainty (1-sigma) in 206Pb/238U age are not included.
2. Analyses with >10% uncertainty (1-sigma) in 206Pb/207Pb age are not included, unless 206Pb/238U age is <500 Ma.
3. Best age is determined from 206Pb/238U age for analyses with 206Pb/238U age <1000 Ma and from 206Pb/207Pb age for analyses with 206Pb/238Uage > 1000 Ma.
4. Concordance is based on 206Pb/238U age / 206Pb/207Pb age. Value is not reported for 206Pb/238U ages <500 Ma because of large uncertainty in 206Pb/207Pb age.
5. Analyses with 206Pb/238U age > 500 Ma and with >20% discordance (<80% concordance) are not included.
6. Analyses with 206Pb/238U age > 500 Ma and with >5% reverse discordance (<105% concordance) are not included.
7. All uncertainties are reported at the 1-sigma level, and include only measurement errors.
8. Systematic errors are as follows (at 2-sigma level): [sample 1: 2.5% (206Pb/238U) & 1.4% (206Pb/207Pb)] These values are reported on cells U1 and W1 of NUagecalc.

Peoria Analysis (sorted by best age)

						Isotope ratios					Apparent ages (Ma)								
Analysis	U	206Pb	U/Th	206Pb*	±	207Pb*	±	206Pb*	±	error	206Pb*	±	207Pb*	±	206Pb*	±	Best age	±	Conc
	(ppm)	204Pb		207Pb*	(%)	235U*	(%)	238U	(%)	corr.	238U*	(Ma)	235U	(Ma)	207Pb*	(Ma)	(Ma)	(Ma)	(%)
Spot 38	20	35813	0.6	13.2183	2.5	1.9317	3.0	0.1852	1.7	0.57	1095.2	17.1	1092.1	20.1	1085.9	49.6	1085.9	49.6	100.9
Spot 40	660	255966	1.5	5.5993	1.6	11.5068	2.5	0.4673	1.9	0.77	2471.7	39.1	2565.1	23.3	2639.8	26.6	2639.8	26.6	93.6
Spot 25	205	61160	4.7	5.5315	1.1	12.6438	2.1	0.5072	1.8	0.85	2644.8	39.3	2653.5	20.0	2660.1	18.4	2660.1	18.4	99.4
Spot 26	542	80655	2.0	5.5158	1.1	12.2759	2.4	0.4911	2.1	0.88	2575.4	44.8	2625.7	22.5	2664.8	18.9	2664.8	18.9	96.6
Spot 12	194	2556728	5.3	5.5058	1.2	13.1350	2.5	0.5245	2.2	0.88	2718.3	48.8	2689.4	23.5	2667.8	19.3	2667.8	19.3	101.9
Spot 1	148	77866	7.0	5.4643	1.4	13.1845	3.0	0.5225	2.6	0.87	2709.8	57.8	2692.9	28.2	2680.3	23.9	2680.3	23.9	101.1
Spot 7	78	143516	8.2	5.4581	1.3	12.8282	2.2	0.5078	1.7	0.81	2647.3	37.9	2667.1	20.4	2682.2	21.2	2682.2	21.2	98.7
Spot 30	191	206574	3.6	5.4521	1.6	12.7439	2.7	0.5039	2.2	0.81	2630.6	47.8	2660.9	25.7	2684.0	26.3	2684.0	26.3	98.0
Spot 11	153	185869	13.5	5.4253	0.9	12.8904	2.3	0.5072	2.1	0.91	2644.7	45.2	2671.7	21.6	2692.1	15.7	2692.1	15.7	98.2
Spot 22	194	139978	5.3	5.4253	1.3	12.7050	2.6	0.4999	2.2	0.86	2613.4	47.0	2658.0	24.1	2692.1	21.8	2692.1	21.8	97.1
Spot 49	119	81073	1.9	5.4227	1.7	13.0970	3.0	0.5151	2.5	0.83	2678.3	54.3	2686.7	28.2	2692.9	27.5	2692.9	27.5	99.5
Spot 31	729	264963	43.7	5.4192	1.0	12.8427	2.5	0.5048	2.3	0.92	2634.2	50.2	2668.2	23.8	2694.0	16.6	2694.0	16.6	97.8
Spot 29	49	171239	1.7	5.4188	1.0	12.9542	2.2	0.5091	2.0	0.89	2652.8	42.4	2676.3	20.6	2694.1	16.2	2694.1	16.2	98.5
Spot 28	270	703824	3.8	5.4142	1.3	13.1231	2.5	0.5153	2.2	0.87	2679.2	48.2	2688.5	24.0	2695.5	21.0	2695.5	21.0	99.4
Spot 17	64	199053	1.7	5.4090	1.5	13.0060	2.5	0.5102	2.0	0.80	2657.6	43.5	2680.1	23.4	2697.1	24.5	2697.1	24.5	98.5
Spot 3	96	148638	1.5	5.4038	1.4	13.2625	2.7	0.5198	2.3	0.86	2698.3	51.4	2698.5	25.5	2698.7	22.6	2698.7	22.6	100.0
Spot 18	760	220984	0.6	5.3965	1.3	10.9280	2.5	0.4277	2.1	0.85	2295.4	41.0	2517.0	23.2	2700.9	21.7	2700.9	21.7	85.0
Spot 47	38	78288	0.6	5.3949	1.2	13.6301	2.4	0.5333	2.0	0.85	2755.4	45.1	2724.4	22.3	2701.4	20.3	2701.4	20.3	102.0
Spot 50	139	90603	3.4	5.3860	1.0	14.0973	2.2	0.5507	2.0	0.89	2828.0	46.0	2756.3	21.3	2704.1	16.7	2704.1	16.7	104.6
Spot 32	435	197959	1.7	5.3815	1.2	12.9734	2.7	0.5064	2.4	0.90	2641.1	52.2	2677.7	25.3	2705.5	19.6	2705.5	19.6	97.6
Spot 15	167	55558	1.4	5.3805	1.1	12.9001	2.3	0.5034	2.1	0.89	2628.4	44.3	2672.4	21.8	2705.8	17.7	2705.8	17.7	97.1
Spot 39	1334	99224	35.1	5.3652	1.4	10.7862	3.5	0.4197	3.2	0.92	2259.2	60.7	2504.9	32.4	2710.5	23.1	2710.5	23.1	83.3
Spot 37	262	75506	1.4	5.3426	1.2	12.7871	2.4	0.4955	2.1	0.86	2594.3	44.2	2664.1	22.6	2717.5	20.0	2717.5	20.0	95.5
Spot 44	486	315745	1.3	5.3416	1.0	13.0180	2.3	0.5043	2.1	0.90	2632.4	45.0	2681.0	21.9	2717.8	17.1	2717.8	17.1	96.9
Spot 2	178	139133	1.6	5.3357	1.4	13.1752	2.7	0.5099	2.3	0.86	2656.0	49.7	2692.3	25.1	2719.6	22.5	2719.6	22.5	97.7
Spot 19	602	980426	6.8	5.3331	1.4	13.4374	2.6	0.5197	2.2	0.85	2698.1	49.3	2710.9	24.9	2720.4	23.0	2720.4	23.0	99.2
Spot 4	116	135617	1.6	5.3300	1.5	13.7124	2.4	0.5301	1.9	0.77	2741.8	41.5	2730.1	22.9	2721.4	25.4	2721.4	25.4	100.7
Spot 36	549	178081	2.4	5.3267	1.4	12.6573	2.8	0.4890	2.5	0.87	2566.3	52.2	2654.5	26.5	2722.4	22.6	2722.4	22.6	94.3
Spot 13	565	132555	11.1	5.3108	1.3	13.4010	2.7	0.5162	2.4	0.88	2682.9	51.6	2708.3	25.4	2727.3	21.3	2727.3	21.3	98.4
Spot 24	210	72022	2.4	5.2949	1.2	13.4050	2.3	0.5148	2.0	0.85	2677.0	43.0	2708.6	21.7	2732.2	19.8	2732.2	19.8	98.0
Spot 46	502	126185	1.9	5.2874	1.2	11.9754	2.4	0.4592	2.0	0.86	2436.1	41.1	2602.5	22.1	2734.6	19.8	2734.6	19.8	89.1
Spot 6	98	115399	4.4	5.2715	1.4	13.4818	2.9	0.5154	2.5	0.87	2679.8	55.5	2714.0	27.5	2739.5	23.4	2739.5	23.4	97.8
Spot 5	202	98024	6.1	5.2614	1.1	13.8965	2.5	0.5303	2.3	0.90	2742.6	51.0	2742.7	24.2	2742.7	18.6	2742.7	18.6	100.0
Spot 34	456	357672	2.1	5.2231	1.1	13.8645	2.3	0.5252	2.0	0.89	2721.2	44.4	2740.5	21.4	2754.7	17.3	2754.7	17.3	98.8
Spot 10	334	184220	2.3	5.2228	1.1	14.1054	2.1	0.5343	1.8	0.85	2759.6	40.7	2756.8	20.2	2754.8	18.5	2754.8	18.5	100.2
Spot 8	64	43624	2.3	5.2143	1.4	13.8510	2.5	0.5238	2.0	0.83	2715.3	45.2	2739.6	23.3	2757.5	22.8	2757.5	22.8	98.5
Spot 20	315	127690	2.4	5.2040	1.1	13.5925	2.0	0.5130	1.7	0.85	2669.5	37.8	2721.7	19.3	2760.7	17.7	2760.7	17.7	96.7
Spot 9	188	187961	2.2	5.1096	1.3	14.3127	2.7	0.5304	2.3	0.87	2743.2	51.6	2770.7	25.2	2790.7	21.5	2790.7	21.5	98.3
Spot 21	78	56606	1.7	5.0999	1.3	14.4174	2.6	0.5333	2.3	0.87	2755.2	51.1	2777.6	25.0	2793.8	21.5	2793.8	21.5	98.6
Spot 35	18	28670	0.5	5.0713	1.7	13.3342	2.7	0.4904	2.1	0.77	2572.6	44.8	2703.6	25.9	2803.1	28.5	2803.1	28.5	91.8
Spot 48	103	154478	1.5	4.9691	1.9	14.8613	4.0	0.5356	3.5	0.89	2765.0	79.7	2806.4	38.1	2836.3	30.3	2836.3	30.3	97.5
Spot 42	52	247861	2.7	4.9506	1.5	15.1867	2.7	0.5453	2.2	0.83	2805.5	50.2	2827.0	25.3	2842.4	24.2	2842.4	24.2	98.7
Spot 43	152	206849	2.3	4.7300	1.0	15.5924	2.1	0.5349	1.8	0.88	2762.1	41.0	2852.2	19.7	2916.4	15.7	2916.4	15.7	94.7
Spot 27	637	136036	2.1	4.4183	1.6	17.9996	2.9	0.5768	2.4	0.83	2935.6	56.8	2989.7	28.1	3026.3	26.4	3026.3	26.4	97.0

Harvard Analysis (sorted by best age)

						Isotope ratios					Apparent ages (Ma)								
Analysis	U	206Pb	U/Th	206Pb*	±	207Pb*	±	206Pb*	±	error	206Pb*	±	207Pb*	±	206Pb*	±	Best age	±	Conc
	(ppm)	204Pb		207Pb*	(%)	235U*	(%)	238U	(%)	corr.	238U*	(Ma)	235U	(Ma)	207Pb*	(Ma)	(Ma)	(Ma)	(%)
Spot 29	797	124647	4.1	5.5092	1.2	11.9542	3.0	0.4776	2.8	0.92	2517.0	58.7	2600.8	28.5	2666.7	19.2	2666.7	19.2	94.4
Spot 31	492	762073	1.4	5.5052	1.2	12.6961	2.5	0.5069	2.2	0.87	2643.5	47.0	2657.4	23.5	2667.9	20.4	2667.9	20.4	99.1
Spot 4	425	299464	6.0	5.4930	0.9	12.3795	1.6	0.4932	1.3	0.83	2584.5	27.3	2633.6	14.6	2671.6	14.5	2671.6	14.5	96.7
Spot 25	283	238927	14.6	5.4909	1.3	12.2594	2.6	0.4882	2.2	0.85	2563.0	46.4	2624.5	24.2	2672.3	22.2	2672.3	22.2	95.9
Spot 22	214	68492	3.0	5.4882	1.3	12.9109	2.5	0.5139	2.2	0.86	2673.3	47.7	2673.2	23.9	2673.1	21.6	2673.1	21.6	100.0
Spot 50	474	91805	2.5	5.4862	1.1	12.1663	2.1	0.4841	1.8	0.85	2545.1	37.5	2617.3	19.6	2673.7	17.9	2673.7	17.9	95.2
Spot 12	66	158850	4.0	5.4834	1.4	12.5616	2.5	0.4996	2.1	0.84	2611.9	45.7	2647.3	23.7	2674.5	22.5	2674.5	22.5	97.7
Spot 8	464	94372	2.0	5.4727	0.8	13.0424	1.4	0.5177	1.2	0.83	2689.3	26.5	2682.7	13.7	2677.8	13.3	2677.8	13.3	100.4
Spot 48	1112	150157	3.4	5.4471	1.8	12.9648	3.7	0.5122	3.2	0.87	2666.0	69.9	2677.1	34.8	2685.5	30.6	2685.5	30.6	99.3
Spot 17	132	411345	2.3	5.4428	1.5	13.3057	2.6	0.5252	2.1	0.82	2721.4	47.7	2701.6	24.7	2686.8	24.5	2686.8	24.5	101.3
Spot 35	781	2373289	1.4	5.4399	1.1	12.6365	2.2	0.4986	1.9	0.86	2607.6	40.3	2652.9	20.7	2687.7	18.8	2687.7	18.8	97.0
Spot 33	173	100882	1.2	5.4373	1.2	12.9033	2.4	0.5088	2.1	0.87	2651.7	45.1	2672.6	22.5	2688.5	19.6	2688.5	19.6	98.6
Spot 10	498	491547	35.1	5.4300	1.4	12.9089	2.4	0.5084	1.9	0.80	2649.7	40.7	2673.0	22.2	2690.7	23.6	2690.7	23.6	98.5
Spot 44	999	637407	4.6	5.4251	1.4	13.6858	2.6	0.5385	2.2	0.85	2777.1	50.6	2728.2	25.0	2692.2	23.0	2692.2	23.0	103.2
Spot 42	441	211186	1.8	5.4225	1.3	13.0601	2.6	0.5136	2.3	0.87	2672.1	49.4	2684.0	24.4	2693.0	20.9	2693.0	20.9	99.2
Spot 46	211	277095	2.1	5.4202	1.4	13.0577	2.8	0.5133	2.5	0.87	2670.7	53.9	2683.8	26.6	2693.7	22.5	2693.7	22.5	99.1
Spot 21	79	58307	1.8	5.4150	1.2	13.2343	2.1	0.5198	1.7	0.82	2698.1	38.4	2696.5	20.1	2695.3	20.3	2695.3	20.3	100.1
Spot 11	203	84803	1.5	5.4135	1.2	12.9140	1.9	0.5070	1.5	0.79	2644.0	33.4	2673.4	18.3	2695.7	19.6	2695.7	19.6	98.1
Spot 47	101	153882	1.7	5.4115	1.4	13.5142	2.6	0.5304	2.2	0.84	2743.2	48.6	2716.3	24.4	2696.3	22.9	2696.3	22.9	101.7
Spot 1	445	77566	0.8	5.3931	1.1	12.9712	2.0	0.5074	1.6	0.82	2645.3	34.9	2677.6	18.5	2702.0	18.6	2702.0	18.6	97.9
Spot 15	262	77739	10.0	5.3923	1.1	12.8330	1.9	0.5019	1.6	0.84	2621.9	34.9	2667.5	18.3	2702.2	17.6	2702.2	17.6	97.0
Spot 5	171	98907	7.5	5.3851	1.0	13.4095	2.1	0.5237	1.9	0.88	2715.0	41.6	2708.9	20.2	2704.4	16.9	2704.4	16.9	100.4
Spot 32	127	67331	1.0	5.3788	1.5	13.4232	3.0	0.5237	2.6	0.87	2714.7	58.0	2709.9	28.4	2706.3	24.4	2706.3	24.4	100.3
Spot 45	301	71822	25.2	5.3780	1.0	13.8315	2.0	0.5395	1.7	0.85	2781.3	38.8	2738.2	19.0	2706.6	17.3	2706.6	17.3	102.8
Spot 49	34	137381	2.1	5.3631	1.6	13.7090	2.6	0.5332	2.1	0.80	2755.1	46.1	2729.8	24.4	2711.2	25.6	2711.2	25.6	101.6
Spot 18	77	131397	2.6	5.3571	1.4	13.9507	2.5	0.5420	2.0	0.83	2791.9	46.4	2746.4	23.3	2713.0	22.5	2713.0	22.5	102.9
Spot 6	280	168556	1.2	5.3568	0.9	13.2607	1.8	0.5152	1.6	0.86	2678.8	34.4	2698.4	17.2	2713.1	15.1	2713.1	15.1	98.7
Spot 34	62	65206	3.0	5.3545	1.3	14.1061	2.5	0.5478	2.2	0.86	2816.0	49.9	2756.9	24.0	2713.8	21.0	2713.8	21.0	103.8
Spot 19	2154	76236	2.3	5.3504	1.7	11.4826	2.9	0.4456	2.3	0.82	2375.6	46.4	2563.2	26.7	2715.1	27.3	2715.1	27.3	87.5
Spot 16	121	726743	1.2	5.3487	1.0	13.7681	2.5	0.5341	2.3	0.91	2758.7	50.9	2733.9	23.7	2715.6	17.3	2715.6	17.3	101.6
Spot 28	157	112745	3.5	5.3457	1.4	13.5619	2.5	0.5258	2.1	0.84	2723.8	47.4	2719.6	24.0	2716.5	22.6	2716.5	22.6	100.3
Spot 9	303	96942	4.4	5.3189	1.2	13.0638	2.2	0.5040	1.9	0.84	2630.8	40.8	2684.3	21.2	2724.8	20.0	2724.8	20.0	96.5
Spot 3	2663	94780	2.6	5.2978	1.1	11.7574	2.2	0.4518	1.9	0.87	2403.1	38.8	2585.3	20.8	2731.4	17.9	2731.4	17.9	88.0
Spot 30	69	147398	1.1	5.2860	1.6	13.7369	2.6	0.5266	2.1	0.80	2727.3	46.5	2731.7	24.6	2735.0	25.6	2735.0	25.6	99.7
Spot 13	354	5132161	1.5	5.2802	1.5	13.5066	2.4	0.5172	1.9	0.79	2687.5	41.7	2715.7	22.6	2736.8	23.9	2736.8	23.9	98.2
Spot 20	172	80043	4.5	5.2759	1.1	13.8409	2.2	0.5296	2.0	0.88	2739.8	44.3	2738.9	21.3	2738.2	17.4	2738.2	17.4	100.1
Spot 43	270	120346	0.7	5.2443	1.1	13.2927	2.6	0.5056	2.4	0.90	2637.8	51.4	2700.7	24.8	2748.0	18.5	2748.0	18.5	96.0
Spot 41	877	38487	5.0	5.2368	1.2	13.7591	2.8	0.5226	2.6	0.91	2710.1	56.8	2733.3	26.7	2750.4	19.1	2750.4	19.1	98.5
Spot 36	130	5100997	1.0	5.2290	1.6	14.3577	2.7	0.5445	2.2	0.81	2802.3	49.9	2773.6	25.6	2752.9	25.8	2752.9	25.8	101.8
Spot 24	1082	170413	16.0	5.1875	1.3	13.5651	2.6	0.5104	2.2	0.87	2658.2	48.7	2719.8	24.4	2765.9	21.3	2765.9	21.3	96.1
Spot 27	104	85344	1.6	5.1531	1.5	14.0141	2.6	0.5238	2.1	0.83	2715.1	47.5	2750.7	24.6	2776.9	23.8	2776.9	23.8	97.8
Spot 2	50	40815	0.4	5.1204	1.0	13.5061	2.4	0.5016	2.1	0.91	2620.5	46.3	2715.7	22.4	2787.3	16.5	2787.3	16.5	94.0
Spot 39	344	29337	3.9	5.0596	1.5	12.3557	2.4	0.4534	1.9	0.78	2410.4	38.0	2631.8	22.6	2806.8	24.4	2806.8	24.4	85.9
Spot 40	689	266079	1.9	5.0012	1.3	15.0550	2.7	0.5461	2.3	0.86	2808.8	52.7	2818.7	25.5	2825.8	22.0	2825.8	22.0	99.4
Spot 14	672	98875	5.5	4.9883	0.9	14.9612	2.0	0.5413	1.8	0.90	2788.8	39.7	2812.8	18.6	2830.0	13.9	2830.0	13.9	98.5
Spot 38	329	92106	5.2	4.7549	1.7	16.1603	3.1	0.5573	2.6	0.84	2855.4	60.3	2886.3	29.8	2907.9	27.4	2907.9	27.4	98.2

Tiskilwa Analysis (sorted by best age)

						Isotope ratios					Apparent ages (Ma)								
Analysis	U	206Pb	U/Th	206Pb*	±	207Pb*	±	206Pb*	±	error	206Pb*	±	207Pb*	±	206Pb*	±	Best age	±	Conc
	(ppm)	204Pb		207Pb*	(%)	235U*	(%)	238U	(%)	corr.	238U*	(Ma)	235U	(Ma)	207Pb*	(Ma)	(Ma)	(Ma)	(%)
Spot 47	259	37604	12.9	6.9959	2.0	6.5782	3.8	0.3338	3.2	0.85	1856.6	52.3	2056.4	33.7	2263.1	35.1	2263.1	35.1	82.0
Spot 28	224	91615	7.2	5.6745	1.3	10.9166	2.4	0.4493	2.0	0.83	2392.0	39.7	2516.1	22.2	2617.7	22.1	2617.7	22.1	91.4
Spot 15	303	34103	1.4	5.6536	2.5	12.3640	3.5	0.5070	2.4	0.70	2643.7	52.2	2632.4	32.4	2623.8	41.2	2623.8	41.2	100.8
Spot 4	23	38017	2.8	5.6185	1.5	12.3875	2.6	0.5048	2.1	0.81	2634.3	45.9	2634.2	24.6	2634.2	25.5	2634.2	25.5	100.0
Spot 29	317	219963	1.9	5.5700	1.2	13.2312	2.5	0.5345	2.2	0.88	2760.4	48.7	2696.3	23.3	2648.5	19.4	2648.5	19.4	104.2
Spot 16	22	61278	3.6	5.5360	1.5	13.4077	2.7	0.5383	2.2	0.82	2776.5	49.5	2708.8	25.4	2658.7	25.6	2658.7	25.6	104.4
Spot 25	60	187378	1.3	5.5150	1.1	13.1443	2.1	0.5257	1.7	0.83	2723.5	37.9	2690.1	19.4	2665.0	18.8	2665.0	18.8	102.2
Spot 50	172	133689	3.1	5.5047	1.5	13.1655	2.4	0.5256	1.9	0.79	2722.9	42.5	2691.6	22.8	2668.1	24.4	2668.1	24.4	102.1
Spot 17	252	63878	2.4	5.5038	1.2	13.0062	2.0	0.5192	1.6	0.80	2695.7	35.7	2680.1	19.1	2668.4	20.1	2668.4	20.1	101.0
Spot 10	183	246104	2.1	5.5023	1.4	12.8416	2.5	0.5125	2.1	0.83	2667.1	46.1	2668.1	23.9	2668.8	23.5	2668.8	23.5	99.9
Spot 45	428	8209787	5.0	5.4900	1.0	13.2369	2.1	0.5271	1.9	0.89	2729.0	42.7	2696.7	20.3	2672.5	16.0	2672.5	16.0	102.1
Spot 44	393	97774	6.6	5.4790	1.0	13.0450	2.5	0.5184	2.3	0.91	2692.3	49.7	2682.9	23.3	2675.8	16.8	2675.8	16.8	100.6
Spot 37	114	81772	5.8	5.4687	1.4	13.2322	2.7	0.5248	2.3	0.86	2719.6	51.0	2696.4	25.3	2679.0	22.8	2679.0	22.8	101.5
Spot 26	634	169520	4.3	5.4642	1.1	12.9843	1.9	0.5146	1.5	0.81	2676.1	33.0	2678.5	17.6	2680.3	18.3	2680.3	18.3	99.8
Spot 30	28	25868	3.7	5.4610	1.5	13.3142	2.5	0.5273	2.0	0.81	2730.2	45.6	2702.2	23.8	2681.3	24.1	2681.3	24.1	101.8
Spot 46	300	149582	2.9	5.4512	1.0	13.2222	1.9	0.5227	1.6	0.85	2710.8	35.6	2695.6	17.9	2684.3	16.5	2684.3	16.5	101.0
Spot 20	489	401566	5.6	5.4504	1.2	13.2822	2.3	0.5250	2.0	0.85	2720.6	43.3	2699.9	21.6	2684.5	19.8	2684.5	19.8	101.3
Spot 49	286	254757	0.6	5.4355	1.2	13.4880	2.1	0.5317	1.8	0.83	2748.7	39.4	2714.4	20.0	2689.0	19.5	2689.0	19.5	102.2
Spot 19	560	607871	5.3	5.4327	0.9	13.1147	2.1	0.5167	1.9	0.90	2685.3	41.9	2687.9	20.1	2689.9	15.7	2689.9	15.7	99.8
Spot 34	445	175288	4.4	5.4289	0.9	13.1434	2.1	0.5175	1.9	0.90	2688.6	41.2	2690.0	19.6	2691.0	15.0	2691.0	15.0	99.9
Spot 3	991	27879	1.4	5.4161	1.0	11.8055	2.5	0.4637	2.3	0.91	2456.0	46.4	2589.1	23.4	2694.9	17.3	2694.9	17.3	91.1
Spot 31	73	66920	4.0	5.4160	0.9	13.8361	2.0	0.5435	1.8	0.90	2798.0	41.1	2738.6	19.0	2695.0	14.4	2695.0	14.4	103.8
Spot 35	384	54966	6.8	5.4025	1.5	12.9159	3.1	0.5061	2.7	0.88	2639.9	59.0	2673.5	29.3	2699.1	24.9	2699.1	24.9	97.8
Spot 12	106	52315	1.2	5.4007	1.4	13.9572	2.7	0.5467	2.4	0.86	2811.4	53.6	2746.8	25.9	2699.6	23.1	2699.6	23.1	104.1
Spot 9	309	107030	2.1	5.3972	1.1	13.1354	1.8	0.5142	1.4	0.79	2674.4	30.8	2689.4	16.8	2700.7	18.1	2700.7	18.1	99.0
Spot 7	493	207324	4.4	5.3922	1.1	13.6864	2.2	0.5352	1.9	0.86	2763.5	41.8	2728.3	20.6	2702.2	18.5	2702.2	18.5	102.3
Spot 14	257	56489	3.7	5.3790	0.9	13.3752	2.3	0.5218	2.1	0.91	2706.8	46.3	2706.5	21.7	2706.3	15.3	2706.3	15.3	100.0
Spot 6	810	67520	14.0	5.3789	1.0	13.4488	2.0	0.5247	1.7	0.87	2718.9	38.3	2711.7	18.9	2706.3	16.5	2706.3	16.5	100.5
Spot 11	600	70298	4.0	5.3758	1.4	12.1873	3.2	0.4752	2.9	0.89	2506.2	59.5	2618.9	30.1	2707.3	23.8	2707.3	23.8	92.6
Spot 41	527	213852	3.5	5.3711	1.2	13.3172	2.8	0.5188	2.5	0.90	2694.0	55.0	2702.4	26.1	2708.7	19.5	2708.7	19.5	99.5
Spot 21	138	119846	13.0	5.3660	1.3	13.0529	2.8	0.5080	2.4	0.88	2648.1	52.9	2683.5	26.2	2710.3	21.9	2710.3	21.9	97.7
Spot 24	1090	99967	2.9	5.3545	0.9	13.2181	2.0	0.5133	1.7	0.89	2670.8	38.2	2695.4	18.5	2713.8	14.6	2713.8	14.6	98.4
Spot 36	217	62743	3.7	5.3461	1.1	14.0673	2.2	0.5454	1.9	0.86	2806.2	42.3	2754.3	20.5	2716.4	18.1	2716.4	18.1	103.3
Spot 27	704	555479	1.0	5.3451	1.1	13.5123	2.1	0.5238	1.8	0.85	2715.4	39.9	2716.1	20.1	2716.7	18.5	2716.7	18.5	99.9
Spot 8	40	42489	0.9	5.3288	0.9	14.1643	2.3	0.5474	2.1	0.91	2814.4	48.0	2760.8	21.9	2721.8	15.5	2721.8	15.5	103.4
Spot 42	199	68151	10.5	5.3268	1.3	13.8950	2.5	0.5368	2.2	0.86	2770.1	48.9	2742.6	23.8	2722.4	21.0	2722.4	21.0	101.8
Spot 43	733	219391	51.0	5.3086	1.2	13.4248	2.7	0.5169	2.4	0.89	2685.9	53.4	2710.0	25.8	2728.0	20.3	2728.0	20.3	98.5
Spot 32	325	1258224	3.6	5.2864	1.2	13.4567	2.5	0.5159	2.2	0.87	2681.9	47.2	2712.3	23.3	2734.9	19.7	2734.9	19.7	98.1
Spot 1	70	87600	2.7	5.2739	1.5	12.1098	2.8	0.4632	2.4	0.85	2453.7	48.5	2612.9	26.3	2738.8	24.5	2738.8	24.5	89.6
Spot 23	381	85081	1.3	5.2036	0.9	13.4757	2.1	0.5086	1.9	0.91	2650.6	42.1	2713.6	20.2	2760.8	14.9	2760.8	14.9	96.0
Spot 48	1046	395097	1.5	5.1868	1.1	13.0495	2.0	0.4909	1.7	0.83	2574.6	35.3	2683.2	18.8	2766.1	18.1	2766.1	18.1	93.1
Spot 39	103	240648	2.2	4.8084	1.1	16.4924	2.0	0.5752	1.7	0.85	2928.9	40.3	2905.8	19.3	2889.8	17.2	2889.8	17.2	101.4
Spot 13	642	435699	3.3	4.6347	1.3	17.4127	2.5	0.5853	2.1	0.85	2970.4	51.1	2957.9	24.3	2949.3	21.8	2949.3	21.8	100.7
Spot 2	620	214768	2.3	4.6162	1.1	17.3981	2.4	0.5825	2.1	0.88	2958.9	50.2	2957.0	23.0	2955.8	18.2	2955.8	18.2	100.1
Spot 38	889	188810	8.2	4.5530	1.1	15.2679	2.4	0.5042	2.1	0.88	2631.7	45.1	2832.1	22.5	2978.0	17.9	2978.0	17.9	88.4
Spot 40	613	54951	1.5	4.5292	1.5	15.9057	2.7	0.5225	2.2	0.84	2709.7	49.2	2871.1	25.4	2986.5	23.5	2986.5	23.5	90.7

Putnam Analysis (sorted by best age)

						Isotope ratios							Apparent ages (Ma)						
Analysis	U	206Pb	U/Th	206Pb*	±	207Pb*	±	206Pb*	±	error	206Pb*	±	207Pb*	±	206Pb*	±	Best age	±	Conc
	(ppm)	204Pb		207Pb*	(%)	235U*	(%)	238U	(%)	corr.	238U*	(Ma)	235U	(Ma)	207Pb*	(Ma)	(Ma)	(Ma)	(%)
Spot 51	120	53188	2.9	12.0518	1.6	2.5756	3.4	0.2251	3.1	0.89	1308.9	36.3	1293.7	25.2	1268.6	30.8	1268.6	30.8	103.2
Spot 52	405	316984	3.3	5.5517	1.1	12.4149	2.2	0.4999	1.9	0.87	2613.3	41.5	2636.3	20.9	2654.0	18.2	2654.0	18.2	98.5
Spot 53	366	2105254	0.7	5.4434	1.7	13.2063	2.7	0.5214	2.1	0.77	2705.0	45.8	2694.5	25.5	2686.6	28.7	2686.6	28.7	100.7
Spot 54	81	77663	1.8	5.2462	1.3	14.1276	2.5	0.5375	2.1	0.85	2773.1	47.5	2758.3	23.5	2747.5	21.5	2747.5	21.5	100.9
Spot 55	203	117825	3.8	5.3637	1.3	13.6174	2.2	0.5297	1.8	0.83	2740.3	41.0	2723.5	21.0	2711.0	20.6	2711.0	20.6	101.1
Spot 56	388	64718	2.5	5.4720	1.6	10.9794	3.5	0.4357	3.1	0.88	2331.5	59.8	2521.4	32.2	2677.9	26.6	2677.9	26.6	87.1
Spot 57	7815	444156	0.0	4.4948	2.2	16.7862	4.6	0.5472	4.1	0.88	2813.6	93.1	2922.7	44.3	2998.7	34.7	2998.7	34.7	93.8
Spot 58	261	167136	3.6	5.3615	0.9	13.2989	2.1	0.5171	1.9	0.91	2687.0	42.3	2701.1	20.1	2711.6	14.8	2711.6	14.8	99.1
Spot 59	472	57804	4.1	5.4143	1.2	12.3418	2.3	0.4846	2.0	0.86	2547.5	41.6	2630.8	21.5	2695.5	19.2	2695.5	19.2	94.5
Spot 60	155	120513	4.8	5.4911	1.3	12.7504	2.7	0.5078	2.3	0.87	2647.2	50.5	2661.4	25.2	2672.2	21.9	2672.2	21.9	99.1
Spot 61	305	676911	2.7	5.3809	1.4	13.2538	2.6	0.5172	2.2	0.83	2687.5	47.4	2697.9	24.5	2705.7	23.7	2705.7	23.7	99.3
Spot 62	117	2101135	5.3	5.4616	1.3	12.5961	2.4	0.4989	2.0	0.85	2609.3	43.4	2649.9	22.4	2681.1	20.7	2681.1	20.7	97.3
Spot 63	400	84253	10.3	5.4664	1.1	13.1033	1.7	0.5195	1.3	0.78	2697.1	29.3	2687.1	16.1	2679.6	17.7	2679.6	17.7	100.6
Spot 64	143	216512	1.0	5.4380	1.3	13.2381	2.7	0.5221	2.4	0.88	2708.1	52.3	2696.8	25.5	2688.3	21.6	2688.3	21.6	100.7
Spot 65	271	58908	3.0	5.2401	1.4	14.7865	2.9	0.5620	2.5	0.87	2874.7	57.9	2801.6	27.2	2749.4	22.9	2749.4	22.9	104.6
Spot 66	1685	343421	10.8	5.3729	1.4	12.6844	2.7	0.4943	2.3	0.86	2589.2	49.5	2656.5	25.5	2708.1	23.0	2708.1	23.0	95.6
Spot 67	234	951374	2.4	5.4285	1.0	13.2119	2.2	0.5202	2.0	0.89	2699.9	43.6	2694.9	21.1	2691.2	17.1	2691.2	17.1	100.3
Spot 68	474	1076048	0.9	5.4344	1.1	13.1440	2.0	0.5181	1.6	0.84	2690.9	36.1	2690.0	18.5	2689.4	17.7	2689.4	17.7	100.1
Spot 69	1637	162284	87.0	5.5445	1.3	9.9212	3.3	0.3990	3.0	0.92	2164.2	55.6	2427.5	30.3	2656.2	21.4	2656.2	21.4	81.5
Spot 70	853	112273	0.6	5.2435	1.4	12.3403	3.0	0.4693	2.6	0.87	2480.5	53.2	2630.6	27.8	2748.3	23.7	2748.3	23.7	90.3
Spot 71	89	122122	1.2	5.2949	1.3	13.3881	2.3	0.5141	1.9	0.82	2674.3	41.2	2707.4	21.8	2732.3	22.0	2732.3	22.0	97.9
Spot 72	247	54851	2.6	5.3420	1.3	13.2972	2.4	0.5152	2.0	0.84	2678.7	44.3	2701.0	22.8	2717.7	21.6	2717.7	21.6	98.6
Spot 73	1836	44592	0.0	5.1010	1.2	14.0301	2.6	0.5191	2.3	0.88	2695.2	50.9	2751.7	24.7	2793.5	19.9	2793.5	19.9	96.5
Spot 74	569	209171	4.3	5.3097	1.2	13.3671	2.7	0.5148	2.4	0.89	2676.9	52.7	2705.9	25.5	2727.7	20.2	2727.7	20.2	98.1
Spot 75	941	119146	4.0	5.4313	1.6	12.5765	3.2	0.4954	2.8	0.87	2594.0	59.5	2648.5	30.1	2690.3	26.2	2690.3	26.2	96.4
Spot 77	1393	186730	164.0	5.5270	1.3	12.0701	2.1	0.4838	1.7	0.81	2544.0	36.7	2609.9	20.2	2661.4	20.7	2661.4	20.7	95.6
Spot 78	597	99198	1.4	5.2879	1.2	12.6760	2.6	0.4861	2.3	0.88	2554.0	47.6	2655.9	24.1	2734.4	19.8	2734.4	19.8	93.4
Spot 79	246	179976	2.2	5.5285	1.4	11.6413	2.3	0.4668	1.8	0.80	2469.4	37.5	2576.0	21.3	2660.9	22.6	2660.9	22.6	92.8
Spot 80	100	101281	2.3	5.4676	1.2	13.1643	2.1	0.5220	1.7	0.82	2707.8	37.5	2691.5	19.5	2679.3	19.6	2679.3	19.6	101.1
Spot 81	596	66449	4.0	5.3588	0.9	13.1158	2.0	0.5098	1.8	0.89	2655.6	38.8	2688.0	19.0	2712.5	15.3	2712.5	15.3	97.9
Spot 83	251	2453763	2.0	5.4857	1.3	12.5515	2.0	0.4994	1.6	0.78	2611.1	33.5	2646.6	18.9	2673.8	21.0	2673.8	21.0	97.7

Genoa Analysis (sorted by best age)

						Isotope ratios							Apparent ages (Ma)						
Analysis	U	206Pb	U/Th	206Pb*	±	207Pb*	±	206Pb*	±	error	206Pb*	±	207Pb*	±	206Pb*	±	Best age	±	Conc
	(ppm)	204Pb		207Pb*	(%)	235U*	(%)	238U	(%)	corr.	238U*	(Ma)	235U	(Ma)	207Pb*	(Ma)	(Ma)	(Ma)	(%)
Spot 13	2275	81075	4.8	5.6346	1.1	10.0541	2.0	0.4109	1.7	0.83	2218.9	31.3	2439.8	18.6	2629.4	18.8	2629.4	18.8	84.4
Spot 45	708	101435	4.7	5.6248	1.3	11.7917	2.3	0.4810	1.9	0.84	2531.8	40.3	2588.0	21.5	2632.3	20.9	2632.3	20.9	96.2
Spot 27	310	113000	1.1	5.5217	1.0	12.5192	1.9	0.5014	1.6	0.85	2619.6	33.8	2644.2	17.4	2663.0	16.4	2663.0	16.4	98.4
Spot 32	141	183196	1.5	5.4677	1.2	12.5951	2.4	0.4995	2.1	0.87	2611.5	45.5	2649.9	22.9	2679.3	19.8	2679.3	19.8	97.5
Spot 31	112	102020	1.3	5.4646	1.4	12.9962	2.6	0.5151	2.2	0.85	2678.3	49.0	2679.4	24.9	2680.2	23.4	2680.2	23.4	99.9
Spot 17	122	211497	4.5	5.4486	1.3	13.0511	2.6	0.5157	2.3	0.87	2681.1	49.6	2683.4	24.4	2685.1	20.9	2685.1	20.9	99.9
Spot 43	414	76907	0.6	5.4423	1.5	12.7840	2.5	0.5046	2.0	0.80	2633.5	42.5	2663.9	23.2	2687.0	24.5	2687.0	24.5	98.0
Spot 23	1131	70423	0.4	5.4420	1.0	10.3503	2.1	0.4085	1.8	0.87	2208.1	33.9	2466.6	19.2	2687.0	16.8	2687.0	16.8	82.2
Spot 19	962	1399420	0.4	5.4329	1.0	12.3940	2.3	0.4884	2.0	0.89	2563.6	42.7	2634.7	21.2	2689.8	16.7	2689.8	16.7	95.3
Spot 7	202	155182	2.4	5.4282	1.0	13.2022	1.8	0.5198	1.6	0.85	2698.2	34.6	2694.2	17.4	2691.2	15.8	2691.2	15.8	100.3
Spot 1	97	84548	1.2	5.4278	1.1	12.7199	2.1	0.5007	1.8	0.85	2617.0	38.3	2659.1	19.7	2691.4	18.1	2691.4	18.1	97.2
Spot 9	180	104374	3.5	5.4268	1.2	12.8109	2.3	0.5042	2.0	0.87	2631.9	43.9	2665.8	22.1	2691.7	19.2	2691.7	19.2	97.8
Spot 29	242	59562	4.0	5.4189	1.3	12.8491	2.2	0.5050	1.8	0.81	2635.2	38.4	2668.7	20.7	2694.1	21.4	2694.1	21.4	97.8
Spot 40	206	62672	3.5	5.4050	1.2	13.3962	2.4	0.5251	2.1	0.87	2720.9	45.7	2708.0	22.3	2698.3	19.0	2698.3	19.0	100.8
Spot 39	228	65109	1.4	5.3941	1.1	12.3732	2.4	0.4841	2.2	0.90	2544.9	46.0	2633.1	22.8	2701.7	17.5	2701.7	17.5	94.2
Spot 26	140	170727	1.2	5.3928	0.8	12.9883	1.7	0.5080	1.5	0.87	2648.1	32.4	2678.8	16.1	2702.1	13.7	2702.1	13.7	98.0
Spot 2	155	370918	1.2	5.3877	1.2	13.1780	2.1	0.5149	1.7	0.83	2677.7	37.3	2692.5	19.5	2703.6	19.2	2703.6	19.2	99.0
Spot 3	25	119583	2.6	5.3762	1.4	13.3487	2.4	0.5205	1.9	0.80	2701.3	41.9	2704.6	22.5	2707.1	23.7	2707.1	23.7	99.8
Spot 10	88	77129	3.2	5.3755	1.1	13.2177	2.1	0.5153	1.8	0.86	2679.3	40.0	2695.3	20.0	2707.4	17.8	2707.4	17.8	99.0
Spot 30	149	160614	3.6	5.3744	1.1	13.3996	1.9	0.5223	1.5	0.81	2708.9	33.5	2708.2	17.7	2707.7	18.1	2707.7	18.1	100.0
Spot 38	90	94037	3.0	5.3728	1.4	13.1260	2.7	0.5115	2.4	0.86	2662.9	51.7	2688.7	25.9	2708.2	22.8	2708.2	22.8	98.3
Spot 28	257	61623	3.0	5.3680	1.4	12.5574	2.2	0.4889	1.8	0.79	2565.9	37.2	2647.0	20.9	2709.7	22.4	2709.7	22.4	94.7
Spot 20	296	71154	1.1	5.3606	1.1	12.3132	3.0	0.4787	2.8	0.93	2521.7	57.5	2628.6	28.0	2711.9	18.6	2711.9	18.6	93.0
Spot 18	100	99102	1.2	5.3390	1.2	12.8965	2.2	0.4994	1.8	0.83	2611.1	38.7	2672.1	20.4	2718.6	19.8	2718.6	19.8	96.0
Spot 6	195	311445	1.8	5.3283	1.4	12.8720	2.2	0.4974	1.7	0.76	2602.7	35.9	2670.3	20.7	2721.9	23.5	2721.9	23.5	95.6
Spot 24	359	51513	1.0	5.3236	1.0	13.3574	2.1	0.5157	1.8	0.87	2681.1	40.0	2705.3	19.8	2723.3	16.9	2723.3	16.9	98.4
Spot 37	273	65371	1.5	5.3210	1.2	13.3173	2.7	0.5139	2.5	0.90	2673.4	53.8	2702.4	25.8	2724.2	19.4	2724.2	19.4	98.1
Spot 33	372	114434	5.3	5.2969	1.2	13.1363	2.2	0.5047	1.8	0.82	2633.8	38.5	2689.5	20.4	2731.6	20.1	2731.6	20.1	96.4
Spot 42	66	98965	1.1	5.2435	1.3	12.9695	2.7	0.4932	2.3	0.87	2584.6	49.8	2677.4	25.5	2748.3	22.2	2748.3	22.2	94.0
Spot 4	330	14286137	1.4	5.2258	1.2	13.9348	1.9	0.5281	1.4	0.75	2733.6	31.2	2745.3	17.6	2753.9	20.2	2753.9	20.2	99.3
Spot 14	1025	161382	4.4	5.1958	1.1	12.8052	1.9	0.4825	1.5	0.81	2538.4	32.0	2665.4	17.7	2763.3	18.0	2763.3	18.0	91.9
Spot 12	693	294083	1.2	5.1695	1.1	14.1466	1.8	0.5304	1.4	0.78	2743.1	30.6	2759.6	16.6	2771.7	18.0	2771.7	18.0	99.0
Spot 35	1078	194712	1.4	5.1279	1.1	13.2342	2.6	0.4922	2.3	0.90	2580.2	49.3	2696.5	24.4	2784.9	18.8	2784.9	18.8	92.6
Spot 15	359	47897	20.7	5.0964	1.2	13.3247	2.0	0.4925	1.7	0.82	2581.6	35.6	2702.9	19.4	2795.0	19.3	2795.0	19.3	92.4
Spot 34	1564	671769	6.4	5.0793	1.6	14.2524	3.5	0.5250	3.1	0.89	2720.5	69.2	2766.6	33.2	2800.5	26.0	2800.5	26.0	97.1
Spot 47	37	29025	0.2	5.0245	1.3	13.4839	2.5	0.4914	2.1	0.84	2576.6	44.3	2714.2	23.5	2818.2	21.9	2818.2	21.9	91.4
Spot 46	27	19926	0.5	4.8884	1.4	13.6248	2.3	0.4831	1.9	0.80	2540.6	39.1	2724.0	22.1	2863.0	23.0	2863.0	23.0	88.7
Spot 22	166	44842	1.2	4.8883	1.2	12.9817	2.3	0.4602	2.0	0.86	2440.7	41.0	2678.3	22.1	2863.0	19.6	2863.0	19.6	85.2

Shelbyville Analysis (sorted by best age)

						Isotope ratios							Apparent ages (Ma)						
Analysis	U	206Pb	U/Th	206Pb*	±	207Pb*	±	206Pb*	±	error	206Pb*	±	207Pb*	±	206Pb*	±	Best age	±	Conc
	(ppm)	204Pb		207Pb*	(%)	235U*	(%)	238U	(%)	corr.	238U*	(Ma)	235U	(Ma)	207Pb*	(Ma)	(Ma)	(Ma)	(%)
Spot 93	138	94995	1.2	12.2433	1.4	2.3364	2.7	0.2075	2.3	0.85	1215.3	25.5	1223.4	19.2	1237.8	27.8	1237.8	27.8	98.2
Spot 78	106	42778	1.6	12.1154	1.7	2.4331	3.0	0.2138	2.5	0.83	1249.0	28.4	1252.4	21.6	1258.4	32.7	1258.4	32.7	99.3
Spot 58	160	65090	2.0	11.8440	1.7	2.5655	3.0	0.2204	2.5	0.83	1283.9	29.4	1290.9	22.2	1302.5	32.6	1302.5	32.6	98.6
Spot 59	47	128901	2.3	5.5600	1.3	12.2326	2.2	0.4933	1.8	0.80	2584.8	38.4	2622.4	21.1	2651.5	22.2	2651.5	22.2	97.5
Spot 89	229	939460	15.5	5.4564	1.1	12.8314	2.4	0.5078	2.2	0.90	2647.2	47.5	2667.3	22.9	2682.7	17.7	2682.7	17.7	98.7
Spot 60	41	43550	2.5	5.4524	1.5	12.8182	2.5	0.5069	2.0	0.80	2643.4	43.0	2666.4	23.3	2683.9	24.4	2683.9	24.4	98.5
Spot 54	94	143329	1.8	5.4511	1.4	12.8727	2.7	0.5089	2.3	0.85	2652.0	49.4	2670.4	25.2	2684.3	23.4	2684.3	23.4	98.8
Spot 91	399	76971	4.8	5.4470	1.5	13.0704	2.4	0.5164	1.9	0.78	2683.7	41.5	2684.7	22.8	2685.5	24.8	2685.5	24.8	99.9
Spot 55	284	802015	2.2	5.4391	1.2	12.5884	2.0	0.4966	1.6	0.80	2599.1	35.0	2649.4	19.3	2687.9	20.4	2687.9	20.4	96.7
Spot 87	60	61535	3.1	5.4391	1.4	12.9653	2.7	0.5115	2.4	0.86	2662.9	51.5	2677.1	25.8	2687.9	22.9	2687.9	22.9	99.1
Spot 70	225	176827	1.0	5.4212	1.2	13.1204	2.3	0.5159	1.9	0.85	2681.7	42.6	2688.4	21.5	2693.4	19.6	2693.4	19.6	99.6
Spot 86	133	261899	4.0	5.4187	1.5	12.8295	2.5	0.5042	2.0	0.81	2631.8	43.8	2667.2	23.6	2694.1	24.2	2694.1	24.2	97.7
Spot 94	194	248684	1.7	5.4183	1.2	12.9206	2.4	0.5077	2.1	0.88	2647.0	46.7	2673.9	23.1	2694.3	19.3	2694.3	19.3	98.2
Spot 96	107	93070	8.2	5.4039	1.3	13.0089	2.2	0.5099	1.7	0.79	2656.0	37.8	2680.3	20.7	2698.7	22.3	2698.7	22.3	98.4
Spot 79	421	1048292	0.8	5.4020	1.3	13.2714	2.3	0.5200	1.9	0.83	2699.0	41.8	2699.1	21.7	2699.2	21.3	2699.2	21.3	100.0
Spot 51	150	111639	2.0	5.4013	1.2	12.6931	2.6	0.4972	2.3	0.89	2601.9	49.5	2657.2	24.6	2699.5	20.0	2699.5	20.0	96.4
Spot 82	33	406181	3.2	5.3977	1.3	13.1023	2.3	0.5129	1.9	0.82	2669.1	41.7	2687.0	22.0	2700.6	22.3	2700.6	22.3	98.8
Spot 66	94	113425	3.9	5.3875	1.3	13.2328	2.8	0.5171	2.5	0.89	2686.7	54.6	2696.4	26.3	2703.7	20.7	2703.7	20.7	99.4
Spot 67	230	112265	1.4	5.3862	1.3	13.1636	2.3	0.5142	1.9	0.83	2674.7	41.4	2691.5	21.6	2704.1	21.3	2704.1	21.3	98.9
Spot 57	87	153619	3.4	5.3788	1.6	13.3280	2.6	0.5199	2.1	0.80	2698.9	46.4	2703.2	25.0	2706.4	26.4	2706.4	26.4	99.7
Spot 56	161	208019	1.5	5.3715	1.3	13.4673	2.8	0.5247	2.5	0.88	2718.9	54.6	2713.0	26.3	2708.6	21.4	2708.6	21.4	100.4
Spot 88	88	152067	4.1	5.3692	1.2	13.1961	2.4	0.5139	2.0	0.86	2673.1	44.3	2693.8	22.2	2709.3	19.7	2709.3	19.7	98.7
Spot 68	367	189335	1.8	5.3692	0.9	13.6002	1.9	0.5296	1.6	0.87	2739.8	36.0	2722.3	17.5	2709.3	15.1	2709.3	15.1	101.1
Spot 61	103	278190	3.8	5.3660	1.5	13.0354	2.5	0.5073	2.1	0.81	2645.1	44.7	2682.2	23.8	2710.3	24.2	2710.3	24.2	97.6
Spot 84	88	123256	2.8	5.3650	1.3	13.5148	2.4	0.5259	2.0	0.83	2724.0	44.5	2716.3	22.7	2710.6	21.9	2710.6	21.9	100.5
Spot 72	89	419892	3.5	5.3446	1.3	13.3430	2.2	0.5172	1.8	0.81	2687.3	39.8	2704.2	21.3	2716.9	22.0	2716.9	22.0	98.9
Spot 76	224	116881	1.4	5.3403	1.3	13.6303	2.3	0.5279	1.9	0.82	2732.7	42.6	2724.4	22.1	2718.2	22.2	2718.2	22.2	100.5
Spot 71	247	206872	1.5	5.3252	1.2	13.4545	2.2	0.5196	1.8	0.83	2697.6	39.9	2712.1	20.6	2722.9	19.9	2722.9	19.9	99.1
Spot 97	104	88904	3.5	5.3223	1.7	13.0685	2.9	0.5045	2.4	0.81	2632.9	51.3	2684.6	27.7	2723.7	28.6	2723.7	28.6	96.7
Spot 65	712	87534	4.5	5.3097	1.5	12.9804	2.7	0.4999	2.2	0.82	2613.2	46.9	2678.2	25.1	2727.7	25.1	2727.7	25.1	95.8
Spot 64	126	180212	3.2	5.3047	1.4	13.4158	2.8	0.5161	2.4	0.86	2682.8	52.8	2709.4	26.5	2729.2	23.6	2729.2	23.6	98.3
Spot 99	461	128374	1.7	5.3022	2.0	13.3765	4.3	0.5144	3.8	0.89	2675.4	83.7	2706.6	40.7	2730.0	32.8	2730.0	32.8	98.0
Spot 85	971	50880	1.7	5.2855	1.1	13.4228	2.2	0.5146	1.9	0.86	2676.0	41.7	2709.9	20.9	2735.2	18.5	2735.2	18.5	97.8
Spot 52	139	149145	2.4	5.2823	1.7	13.6966	3.2	0.5247	2.7	0.84	2719.2	58.9	2729.0	29.8	2736.2	27.9	2736.2	27.9	99.4
Spot 100	499	146592	8.0	5.2796	1.2	12.5512	3.3	0.4806	3.1	0.94	2529.9	64.5	2646.6	31.0	2737.0	19.0	2737.0	19.0	92.4
Spot 75	660	135188	3.5	5.2714	1.3	12.6144	2.3	0.4823	2.0	0.84	2537.1	41.1	2651.3	22.0	2739.6	20.9	2739.6	20.9	92.6
Spot 98	228	128531	2.3	5.2548	1.4	13.2224	2.2	0.5039	1.7	0.76	2630.6	36.3	2695.7	20.9	2744.8	23.7	2744.8	23.7	95.8
Spot 74	287	75458	2.0	5.2520	1.3	13.2426	2.5	0.5044	2.2	0.86	2632.8	47.3	2697.1	24.0	2745.6	21.1	2745.6	21.1	95.9
Spot 90	67	128999	2.1	5.2469	1.7	13.7591	2.4	0.5236	1.7	0.71	2714.4	38.3	2733.3	23.1	2747.2	28.4	2747.2	28.4	98.8
Spot 92	466	237877	5.6	5.2419	1.5	13.3075	2.8	0.5059	2.4	0.85	2639.2	51.9	2701.7	26.6	2748.8	24.3	2748.8	24.3	96.0
Spot 63	116	241164	1.4	5.2301	1.1	13.6086	2.0	0.5162	1.7	0.83	2683.1	36.6	2722.9	19.1	2752.5	18.7	2752.5	18.7	97.5
Spot 62	241	54936	2.6	5.2282	1.4	13.6918	2.6	0.5192	2.2	0.85	2695.7	49.5	2728.6	25.1	2753.1	23.1	2753.1	23.1	97.9
Spot 80	219	355549	2.1	5.2262	1.3	14.0117	2.7	0.5311	2.3	0.87	2746.1	51.4	2750.5	25.1	2753.7	21.7	2753.7	21.7	99.7
Spot 73	250	176559	2.1	5.2133	1.4	13.9139	2.5	0.5261	2.1	0.83	2725.0	46.7	2743.9	23.9	2757.8	22.8	2757.8	22.8	98.8
Spot 69	228	114565	2.0	5.2113	1.0	13.6904	1.9	0.5174	1.6	0.84	2688.3	34.8	2728.5	17.8	2758.4	16.8	2758.4	16.8	97.5
Spot 95	514	77215	5.3	5.2102	1.1	13.4337	2.7	0.5076	2.4	0.91	2646.5	52.4	2710.6	25.2	2758.8	18.5	2758.8	18.5	95.9
Spot 83	586	186875	19.8	5.1924	1.1	14.0036	2.3	0.5274	2.0	0.88	2730.3	44.9	2750.0	21.7	2764.4	17.6	2764.4	17.6	98.8
Spot 53	639	25858	5.5	4.9991	1.2	14.0224	2.6	0.5084	2.3	0.89	2649.8	50.9	2751.2	25.0	2826.5	19.7	2826.5	19.7	93.7
Spot 77	153	21555	4.1	4.7129	1.4	15.4446	2.4	0.5279	2.0	0.81	2732.7	43.9	2843.1	23.2	2922.3	23.1	2922.3	23.1	93.5

Charleston Analysis (sorted by best age)

					Isotope ratios						Apparent ages (Ma)								
Analysis	U	206Pb	U/Th	206Pb*	±	207Pb*	±	206Pb*	±	error	206Pb*	±	207Pb*	±	206Pb*	±	Best age	±	Conc
	(ppm)	204Pb		207Pb*	(%)	235U*	(%)	238U	(%)	corr.	238U*	(Ma)	235U	(Ma)	207Pb*	(Ma)	(Ma)	(Ma)	(%)
Spot 78	981	110804	2.2	5.7320	1.4	9.7539	3.0	0.4055	2.6	0.88	2194.3	48.7	2411.8	27.4	2600.9	23.7	2600.9	23.7	84.4
Spot 51	906	100344	0.7	5.7115	1.5	12.0478	2.5	0.4991	2.0	0.79	2609.8	42.3	2608.1	23.2	2606.9	25.0	2606.9	25.0	100.1
Spot 75	4927	94250	53.8	5.6642	1.2	9.9592	2.5	0.4091	2.2	0.89	2210.9	41.7	2431.0	23.2	2620.7	19.2	2620.7	19.2	84.4
Spot 74	111	149300	0.4	5.6587	1.5	11.9472	2.6	0.4903	2.1	0.83	2572.1	45.4	2600.3	24.2	2622.3	24.2	2622.3	24.2	98.1
Spot 99	724	8223519	3.6	5.6497	1.3	12.6172	3.0	0.5170	2.7	0.90	2686.4	58.4	2651.5	27.9	2625.0	21.8	2625.0	21.8	102.3
Spot 52	682	221282	6.2	5.5896	1.2	11.9151	2.6	0.4830	2.3	0.89	2540.5	49.0	2597.8	24.6	2642.7	20.0	2642.7	20.0	96.1
Spot 80	128	79885	0.8	5.5773	1.5	12.5223	2.6	0.5065	2.2	0.83	2641.8	47.7	2644.4	24.9	2646.4	24.3	2646.4	24.3	99.8
Spot 97	375	174065	3.1	5.5656	0.9	12.2288	2.2	0.4936	2.1	0.92	2586.3	43.8	2622.1	20.9	2649.9	14.3	2649.9	14.3	97.6
Spot 90	63	65622	1.4	5.5484	1.4	12.4655	2.4	0.5016	2.0	0.82	2620.7	42.1	2640.1	22.4	2655.0	22.7	2655.0	22.7	98.7
Spot 93	101	45279	1.3	5.5299	1.9	12.6294	3.0	0.5065	2.4	0.78	2641.8	51.0	2652.4	28.3	2660.5	31.1	2660.5	31.1	99.3
Spot 53	1761	74602	1.2	5.5195	1.2	10.6477	2.4	0.4262	2.1	0.87	2288.7	40.4	2492.9	22.3	2663.7	19.4	2663.7	19.4	85.9
Spot 62	200	93636	1.5	5.5164	1.3	12.6250	2.3	0.5051	1.9	0.82	2635.7	40.7	2652.1	21.5	2664.6	21.5	2664.6	21.5	98.9
Spot 60	147	198003	0.8	5.5059	1.6	12.4238	2.4	0.4961	1.8	0.74	2597.1	37.5	2637.0	22.1	2667.7	26.0	2667.7	26.0	97.4
Spot 57	318	171725	0.7	5.4990	1.4	12.7269	2.3	0.5076	1.8	0.81	2646.3	40.0	2659.6	21.5	2669.8	22.4	2669.8	22.4	99.1
Spot 84	978	62429	12.0	5.4927	1.5	11.4149	2.5	0.4547	2.0	0.81	2416.3	40.9	2557.6	23.4	2671.7	24.2	2671.7	24.2	90.4
Spot 96	1322	50886	47.1	5.4798	1.5	13.4267	3.3	0.5336	2.9	0.89	2756.7	64.7	2710.1	30.8	2675.6	25.0	2675.6	25.0	103.0
Spot 68	133	160390	0.9	5.4756	1.5	12.8341	3.3	0.5097	2.9	0.89	2655.2	63.5	2667.6	30.8	2676.9	24.3	2676.9	24.3	99.2
Spot 58	521	166251	1.3	5.4730	1.1	12.2038	2.2	0.4844	1.9	0.86	2546.5	40.2	2620.2	20.8	2677.6	18.6	2677.6	18.6	95.1
Spot 98	190	196755	1.2	5.4651	1.4	11.9460	2.7	0.4735	2.3	0.86	2498.9	48.1	2600.2	25.3	2680.1	22.9	2680.1	22.9	93.2
Spot 91	192	585846	1.5	5.4631	1.4	12.8080	2.6	0.5075	2.2	0.85	2645.9	48.3	2665.6	24.8	2680.6	23.2	2680.6	23.2	98.7
Spot 61	620	233763	19.3	5.4559	1.5	11.7201	4.0	0.4638	3.6	0.92	2456.1	74.3	2582.3	37.0	2682.9	25.6	2682.9	25.6	91.5
Spot 70	1270	203565	1.4	5.4510	1.7	12.1763	3.0	0.4814	2.5	0.83	2533.3	52.1	2618.1	28.2	2684.3	27.8	2684.3	27.8	94.4
Spot 55	1209	115663	2.8	5.4504	1.2	12.9049	2.9	0.5101	2.6	0.91	2657.2	56.9	2672.7	27.2	2684.5	20.3	2684.5	20.3	99.0
Spot 81	101	121398	2.5	5.4190	1.5	12.9774	2.8	0.5100	2.3	0.85	2656.8	50.8	2678.0	26.0	2694.1	24.3	2694.1	24.3	98.6
Spot 94	81	69953	2.1	5.4070	1.5	13.1272	3.3	0.5148	2.9	0.89	2677.0	63.9	2688.8	30.8	2697.7	24.1	2697.7	24.1	99.2
Spot 82	135	1236256	3.0	5.3890	1.2	13.6597	2.2	0.5339	1.9	0.84	2757.8	41.7	2726.4	21.0	2703.2	20.1	2703.2	20.1	102.0
Spot 63	560	292035	3.3	5.3868	1.3	13.4268	2.6	0.5246	2.3	0.88	2718.5	50.7	2710.1	24.7	2703.9	20.9	2703.9	20.9	100.5
Spot 100	1037	222739	0.2	5.3844	1.3	12.3128	3.1	0.4808	2.8	0.90	2530.9	57.7	2628.5	28.8	2704.6	22.1	2704.6	22.1	93.6
Spot 85	851	380378	5.5	5.3813	1.5	12.8027	3.3	0.4997	3.0	0.90	2612.4	63.7	2665.2	31.2	2705.6	24.4	2705.6	24.4	96.6
Spot 65	432	75008	2.8	5.3785	1.2	13.2853	2.5	0.5182	2.1	0.86	2691.7	47.0	2700.1	23.3	2706.4	20.5	2706.4	20.5	99.5
Spot 56	168	50747	2.8	5.3750	1.0	12.8340	2.2	0.5003	1.9	0.88	2615.1	40.9	2667.5	20.5	2707.5	17.3	2707.5	17.3	96.6
Spot 66	178	110130	1.5	5.3691	1.5	12.1444	2.9	0.4729	2.5	0.86	2496.3	51.6	2615.6	27.1	2709.3	24.1	2709.3	24.1	92.1
Spot 64	609	79660	1.7	5.3664	1.3	12.2726	2.2	0.4777	1.8	0.82	2517.0	37.0	2625.5	20.4	2710.2	20.7	2710.2	20.7	92.9
Spot 86	395	100254	2.6	5.3384	1.2	13.1159	2.1	0.5078	1.7	0.83	2647.3	37.7	2688.0	19.8	2718.8	19.3	2718.8	19.3	97.4
Spot 87	114	165788	1.8	5.3248	1.2	13.7673	2.3	0.5317	2.0	0.86	2748.5	43.9	2733.8	21.7	2723.0	19.5	2723.0	19.5	100.9
Spot 73	140	39841	1.0	5.2907	1.3	14.3614	2.5	0.5511	2.2	0.86	2829.6	50.1	2773.9	24.1	2733.6	21.4	2733.6	21.4	103.5
Spot 69	798	159437	1.4	5.2846	1.0	13.4347	2.5	0.5149	2.3	0.92	2677.6	49.8	2710.7	23.4	2735.5	16.1	2735.5	16.1	97.9
Spot 88	176	114955	2.8	5.2654	0.9	14.2873	2.3	0.5456	2.1	0.92	2806.9	48.7	2769.0	22.0	2741.4	14.8	2741.4	14.8	102.4
Spot 83	754	79751	5.7	5.2576	1.8	12.4936	3.4	0.4764	2.8	0.84	2511.6	59.0	2642.2	31.6	2743.9	29.6	2743.9	29.6	91.5
Spot 79	862	47179	10.5	5.2409	1.1	11.9283	2.6	0.4534	2.4	0.90	2410.3	47.5	2598.8	24.5	2749.1	18.6	2749.1	18.6	87.7
Spot 95	71	74893	1.4	5.2364	1.3	13.7364	2.5	0.5217	2.0	0.84	2706.3	45.3	2731.7	23.2	2750.5	22.1	2750.5	22.1	98.4
Spot 77	188	33757	0.4	5.2327	1.6	13.1501	3.2	0.4991	2.8	0.87	2609.8	60.9	2690.5	30.7	2751.7	26.0	2751.7	26.0	94.8
Spot 71	222	192798	1.5	5.0883	1.5	13.9957	2.4	0.5165	1.9	0.78	2684.3	40.9	2749.4	22.5	2797.6	24.2	2797.6	24.2	96.0
Spot 72	216	60072	1.5	5.0333	1.0	14.6402	2.0	0.5344	1.7	0.87	2760.1	38.8	2792.1	18.9	2815.4	15.9	2815.4	15.9	98.0
Spot 54	116	31965	0.9	5.0266	2.7	13.9152	3.3	0.5073	1.8	0.56	2645.1	39.9	2744.0	30.9	2817.5	44.0	2817.5	44.0	93.9
Spot 89	660	111798	1.0	4.9578	1.5	14.9336	3.1	0.5370	2.7	0.87	2770.8	60.1	2811.0	29.3	2840.0	25.1	2840.0	25.1	97.6
Spot 59	194	26386	1.3	4.9346	2.0	12.4024	3.7	0.4439	3.1	0.84	2367.9	62.2	2635.4	35.0	2847.7	32.5	2847.7	32.5	83.2